ENTROPY ANALYSIS DUE TO FREE CONVECTION FLOW ALONG A VERTICAL SURFACE

Thesis Submitted By

Taqwa Kiani

(01-248202-010)

Supervised By

Dr. Rizwan ul Haq

A thesis submitted in fulfilment of the requirements for the award of degree of Masters of Mathematics

Department of Computer Science

BAHRIA UNIVERSITY ISLAMABAD

Session (2020-2022)

Approval of Examination

Scholar Name: Taqwa Kiani

Registration Number: 71101

Enrollment: 01-248202-010

Program of Study: MS Mathematics

Thesis Tittle: Entropy analysis due to free convection flow along a vertical surface.

It is to certify that the above scholar's thesis has been completed to my satisfaction and, to my belief, its standard is appropriate for submission for examination. I have also conducted plagiarism test of this thesis using HEC prescribed software and found similarity index **16%**. That is within the permissible limit set by the HEC for the MS/M.Phil degree thesis. I have also found the thesis in a format recognized by the BU for the MS/M.Phil thesis.

Principal Supervisor Name: Dr. Rizwan ul Haq

Principal Supervisor Signature:

Date: 20-09-2022

Author's Declaration

I, **TAQWA KIANI** hereby state that my MS/MPhil thesis titled **"Entropy analysis due to free convection flow along a vertical surface"** is my own work and has not been submitted previously by me for taking any degree from this university Bahria University or anywhere else in the country/world. At any time if my statement is found to be incorrect even after my Graduate the university has the right to withdraw/cancel my MS/MPhil degree.

Name of student: **Taqwa Kiani**

Date: September 20, 2022

Plagiarism Undertaking

I, **Taqwa Kiani** solemnly declare that research work presented in the thesis titled **"Entropy analysis due to free convection flow along a vertical surface"** is solely my research work with no significant contribution from any other person. Small contribution / help wherever taken has been duly acknowledged and that complete thesis has been written by me. I understand the zero tolerance policy of the HEC and Bahria University towards plagiarism. Therefore I as an Author of the above titled thesis declare that no portion of my thesis has been plagiarized and any material used as reference is properly referred / cited.

I undertake that if I am found guilty of any formal plagiarism in the above titled thesis even after award of MS/MPhil degree, the university reserves the right to withdraw / revoke my MS/MPhil degree and that HEC and the University has the right to publish my name on the HEC / University website on which names of students are placed who submitted plagiarized thesis.

Name of student: **Taqwa Kiani**

Date: September 20, 2022

Dedication

My beloved parents and respected teachers

I dedicate this thesis to my loved ones and revered professors for their unwavering support and participation in helping me succeed in life.

Acknowledgments

Salutations to Almighty Allah, the Lord of the world, the Provider of answers to prayers, the Source of harmony, whose gift and acclaim flourished in the fearful fullness of knowledge. This difficult task was undoubtedly made possible with Allah's help. Honor and reverence for his last messenger, the Holy Prophet Hazrat Muhammad (PBUH). I am the light, the Heavenly Prophet declared, and no one who follows me will ever be in the darkness.

I am pleased to express my sincere gratitude to my kind, devout mentor Dr. Rizwan ul Haq for his unreplaceable leadership, profound insight, affection, and dynamic co-activity that made it possible for this work to be completed successfully and on schedule. Teachers like him are incredibly important resources for rural living for individuals and entire nations. These instructors contribute to a nation's thickness. I am happy that my mentor is also an instructor because it makes working with him unique for me.

I would likewise offer my thanks to all educators. Because of their direction and help am ready to get the outcome of arriving at my objective. The unmistakable among them are Dr. Muhammad Ramzan and Dr. Jafar Husnain, who upheld me in all course fill in and in the fulfillment of this postulation. I thank all regarded educators at the Department of Mathematics, Bahria University Islamabad Campus, for giving us a sound scholarly climate.

I offer my thanks to my relative who gave me each upright and monetary during my review at Bahria University. Accordingly, I had the option to achieve the center errand of the proposal. Without their constant assistance, I was unable to envision accomplishing this objective. I'm additionally appreciative to my companions who gave me each help during my review, Tabinda Sajjad, Ali Raza, and Syed Saqib Ali shah. Toward the end, I would recognize the precious minutes with all my colleagues.

Abstract

This thesis primary goal is to assess how free convection flow along a vertical surface affects the entropy analysis. The assessment is divided into five chapters. The irreversibility of free or forced convection in the presence or absence of nanoparticles is covered in detail in the first chapter in both major and minor features. In the second chapter, fundamental fluid definitions, ideas, and laws have been covered. A review of an article on entropy generation over MHD mixed convection flow inside an inclined stretched sheet is found in the third chapter. The correct tensor is used to generate the governing equations for continuity, momentum, and Temperature. These equations are then transformed into dimensionless form via similarity transformation and numerically solved. The fourth chapter extends the third chapter and applies thermal radiation during convection while considering nanofluid particles and form parameters using the KKL model. Graphs are used to illustrate how Velocity, Temperature, Bejan number, and entropy generation number are affected by the magnetic field, convection, shape parameter, temperature parameter, and Prandtl number. In chapter five, the conclusion is written.

TABLE OF CONTENTS

LIST OF TABLES

LIST OF FIGURES

NOMENCLATURE

V	Velocity field
u, v	Velocity Components
T	Fluid Temperature
T	Time
a, b	Constants
B_o	Uniform magnetic field
g	Gravitational force
C_p	Particular heat at perpetual pressure
q_r	Radiative flux
k	Thermal conductivity
μ_{nf}	Nanofluid dynamic viscosity
μ_f	Kinematic viscosity
k_{nf}	Nanofluid thermal conductivity
$(C_p)_{nf}$	Nanofluid particular heat
ρ_{nf}	Nanofluid density
M	Magnetic field
B_{nf}	Nanofluid thermal expansion
B_f	Thermal expansion
${S_{gen}}'''$	Entropy rate
${S_o}'''$	Volumatic Entropy
Pr	Prandtl number
Ec	Eckert number
Be	Bejan number
Ns	Dimensionless Entropy
Re_x	Reynold number
C_f	Skin friction
$\breve{K}$	Absorption coefficient
$\breve{\sigma}$	Stefan Boltzmann constant
q_w	Heat flux
τ_w	Shear stress
Ω	Temperature parameter
λ	Mixed convection parameter
m	Shape parameters

T_∞	Fluid Temperature deviation from plate
T_w	Fluid Temperature at surface

CHAPTER 1

INTRODUCTION AND LITERATURE REVIEW

Free convection is a form of heat transfer when mass convection or transmission is caused by self-imposed intensity. The gradient in Temperature and concentration may be the intensity source in this particular example. In this overview, we focus on the free convection flow and the heat transfer caused by temperature gradients. Given the presumption above, it should be intuitively evident that buoyancy flow and heat transfer will be closely related. Convection heat transmission will be several times greater than molecular conduction heat transfer because of mass motion. Despite this, because no external force such as a pump or blower is involved in free convection, the velocities will be low, often on the order of cm/s or tens of cm/s, rather than the several m/s seen in forced convection. As a result, free convection heat transfer rates will increase. During the past coral, we have seen significant concern in buoyancy handled convection flow along a vertical surface. Its vast applications mainly include colligative properties, ebullition, solidification, hydrostatic pressure, isotonic pressure, electrolysis, nuclear reactors, aerospace, etc. On the whole, this is as its vast demand for natural and industrial activity.

Entropy generation minimization evaluates the quality of Energy that is nonexistent to any work. The entropy generation's basic concern is thermodynamics irreversibility, which is casual in all heat transfer procedures. Liability of Entropy is countable in different categories of irreversibility, including transfer of heat in a definite temperature gradient, transfer of heat in convection, magnetic flux density, etc. Bejan [1, 2] acknowledges that minimization of irreversibility can be possible if specify the framework of any convection flow in the heat transfer process. The amount of Energy and transformation from one formation to another without a deduction to status, according

to the first law of thermodynamics. Engineers' primary research is on maintaining features and the impact of energy loss on process flow. Cengel et al. [3] indicate that due to the presence of Entropy, lessens the status/quality of Energy. As entropy generation lessens the effectiveness of work, so it is essential to control the entropy generation to enhance the performance of the method. Earliest Erbay et al. [4] state that in the process of flow, diffusive Entropy can be computed and accompanied by other research [5, 6].

Similarly, Komurgoz et al. [7] predicament in an inclined porous channel that there is a magnetic effect on entropy generation. It is concluded that the entropy generation can be maximal in lack of magnetic effect. Rashidi et al. [8] provide evidence of the presence of MHD effect in nanofluid over a pivot porous which generates Entropy. This initiate that pivot porous is the reason behind entropy generation. Butt and Ali [9] explain the irreversibility with heat radiant on unsteady convection magnetohydrodynamic flow in vertical channel.

Convection is the unique or two-phase fluid flow that happens voluntarily. When mixed convection flow occurs in nanoparticles, literature observes the interest in the field. Afridi et al. [10] report Entropy in mixed convection flow. Many other researchers worked on augmenting heat transfer due to convection [11, 12]. Fluid in which nano-size particles with 1-100nm length are suspended is called nanofluid. Nanoparticles have more significant potential to enhance heat transfer (conduction and convection). Choi [13] was the first to use the word nanofluids, which originated from the suspension of nanoparticles. Later on, it was analyzed that a new type of tabulator in the aspect of nanofluid counting entropy generation. [14] explores the numerical simulations of nanofluids in three dimensions with mixed convection. Recently Sheikholeslami et al. [15] worked on thermal entropy analysis.

In addition, nanoparticles change the characteristic of the fluid, and other assumptions that take place in the fluid flow [16, 17, 18] are the ones that show the change in behavior of nanofluids in the presence of nanoparticles. Later on, Mehmood et al. [19] and Iqbal et al. [20] also compline the result of assumptions, including heat source, MHD, and viscous dissipation effect on the surface of stretching sheet. The effect of nanoparticles plays a

vital role in the thermal conductivity of the fluid flow of nanofluid [21]. Some of the researchers used Entropy to check the performance of work [22, 23, 24, 25, 26, 27, 28] – [28]. Recently Shafee et al. [29] studied the Entropy in nanofluid passing through a tube. The nonlinear development of nanoparticles in the liquid is Brownian movement which is gotten from the movement of the particles of liquid. The nonlinear movement of liquid is because of the place of nanoparticle inside the sub-area of liquid. Warm balance of liquid is characterized by this movement through its Temperature. Liquid additionally stay direct all time on account of the Brownian movement. After the botanist Robert Brown, this movement of the nanoparticle is named as Brownian movement. In 1905, Albert Einstein characterized this Brownian development in his paper, and his paper made a tremendous commitment to science [30, 31].

Thermal radiation is supposed to be the method by which a warmed surface discharges Energy as electromagnetic radiation all through all directions. Radiation is the cycle through which Energy is communicated across the material as waves or particles. Radiation is ordered into three types: sound, Energy, and light. Warm radiations are utilized to calculate energy moves in the development of polymers and petroleum derivatives and astrophysical motions. Thermal radiation is fundamental in space investigation, high-temperature activities, and managing the warming system inside that modern polymer area, among different applications. Most researchers demonstrate the effects of nanofluid over free- or forced-convection flow over a stretching sheet surface when heat radiation is present. [32, 33, 34, 35, 36, 37] – [38].

Based on the above investigations, our goal is to use the KKL model with shape effects in the presence of thermal radiation and slip conditions along the vertical surface of the stretching sheet. Also, viscous dissipation is included during the convection process. The numerical solution has been found for Velocity and Temperature. Discussion of all review and extended work is mentioned in chapters 3 and chapter 4, respectively. Lastly, the conclusion of this thesis is in the last chapter.

CHAPTER 2

BASIC DEFINITION AND CONCEPTS

This chapter will discuss the basic definition, concepts, laws, convection, and Entropy.

2.1 Fluid

A substance that has no specific shape and is capable of flowing. A fluid can be liquid, vapor, or gas, for example, oxygen, milk, petrol, etc.

2.2 Classification of fluid:

2.2.1 Ideal Fluid

The fluid has zero viscous, incompressible, and no surface tension. For example gases and smoke etc.

2.2.2 Real Fluid

These fluids have some friction and viscosity effects. They are also compressible. For example petrol and honey etc.

2.3 Fluid Mechanics

It deals with the study of flow and forces in fluids.

2.4 Classification of Fluid Mechanics:

2.4.1 Fluid Static

It deals with the fluids which are under rest.

2.4.2 Fluid Kinematics

Explanation of fluids that have Velocity and acceleration or motion in any fluid particle.

2.4.3 Fluid Dynamics

It studies forces that affect fluid flow's motion or deformation.

2.5 Physical Properties of fluid

It defines a fluid and its behavior in vital applications.

2.5.1 Pressure

The normal force which is applied to the fluid as per area is known as pressure. It is represented as:

$$Pressure = \frac{Force}{Area}.$$

2.5.2 Density

It provides information regarding a substance's physical property, which depends on temperature pressure. It is donated byρ and represented as:

$$\rho = \frac{mass}{volume}.$$

2.5.3 Viscosity

Investigation of fluid thickness is known as viscosity. It is donated by μ and represented as:

$$\mu = \frac{shear\ stress}{rate\ of\ deformation}.$$

2.6 Convection

Convection is the process of transferring heat from a solid to a moving liquid at a different temperature. Convection heat transfer can be:

2.6.1 Free Convection

It results from buoyant forces brought on by density changes brought on by fluid temperature variations.

2.6.2 Forced Convection

Specifically designed to improve heat transmission, this heat transfer method involves forcing fluids to move.

2.6.3 Mixed Convection

It is the combination of forced and natural convection that acts together to transfer heat. Here both pressure and buoyant forces interact.

2.7 Nanofluids

Nature is full of nanofluids, a combination of 100nm particles and base fluid. Nanoparticle materials include: metals, on-metals, etc., and base fluids include: water, oil, etc. These fluids can also be Newtonian and non-Newtonian.

2.8 Thermal radiation

Without using a medium to transfer heat from one location to another. In gases, liquids, and solids, thermal radiation takes place. The three primary ways to transmit heat are convection, conduction, and radiation.

2.9 Entropy generation

A structure's Entropy typically increases due to irreversible processes like erosion, blending, substance reactions, heat transfer through a slight temperature contrast, excessive extension, and pressure. Entropy age is a percentage of the Entropy produced by these impacts throughout a cycle.

According to the second law of thermodynamics, the universe's Entropy increases due to all spontaneous processes.

"Entropy of a pure crystalline substance at absolute zero temperature (zero Kelvin) is zero since the state of each molecule is known," according to the third law of thermodynamics.

2.10 Viscous Dissipation

An irreversible process in which a liquid is incorporated into adjacent layers by the action of shear forces converted into heat is defined as tough scattering.

2.11 Some valid non-dimensional numbers

2.11.1 Reynolds number

A dimensionless metric known as the Reynolds number is defined as the ratio of inertia forces to viscous forces. Mathematically it is represented as:

$$Re = \frac{inertia\ force}{viscous\ forces} = \frac{uL}{\nu}.$$

2.11.2 Prandtl number

It is the ratio of viscous diffusion rate to thermal diffusion rate. It defines specific heat viscosity over thermal conductivity and is also a dimensionless parameter. It is represented as:

$$Pr = \frac{viscous\ diffusion\ rate}{thermal\ diffusion\ rate} = \frac{\mu C_p}{k}.$$

2.11.3 Eckert number

Investigation of flow velocity in specific heat between fluid flows is known as dimensionless parameter Eckert number. Mathematically it can be written as:

$$Ec = \frac{mass\ transport}{heat\ dissipation} = \frac{u^2}{C_p \Delta T}.$$

2.11.4 Nusselt number

The combination of convection and conduction of heat transfer is defined in a dimensionless parameter known as the Nusselt number. It is represented as:

$$Ns = \frac{convection}{conduction} = \frac{hL}{k_f}.$$

2.11.5 Bejan number

Thermodynamics defines it as the proportion of fluid friction's overall irreversibility to the irreversibility of heat transfer. Which, depending on the circumstances of fluid flows, comprises conductive, viscous, and magnetic irreversibility. It is represented as:

$$Be = \frac{conductive + viscous + magnetic + \cdots irrersibility}{Total\ irreversibility}.$$

CHAPTER 3

AN ENTROPY GENERATION OVER MHD MIXED CONVECTION FLOW WITHIN AN INCLINED STRETCHING SHEET

This chapter's primary goal is to investigate the irreversibility of MHD boundary layer flow when mixed convection is present over an inclined stretched surface. The governing equations for boundary layer flow are first formulated. To solve the momentum and energy equations, apply similarity variables and transform the nonlinear PDEs to the dimensionless nonlinear ODEs. It is possible to observe new parameters for momentum and Energy. This chapter is the review of [10].

3.1 Formulation of the Problem

Assuming a steady, two-dimensional flow impeded by an inclined stretched sheet, $u_w(x) = cx$ linear Velocity is, and B_o is the magnetic field normally applied to the sheet. The respective governing equation of continuity and momentum take the following form:

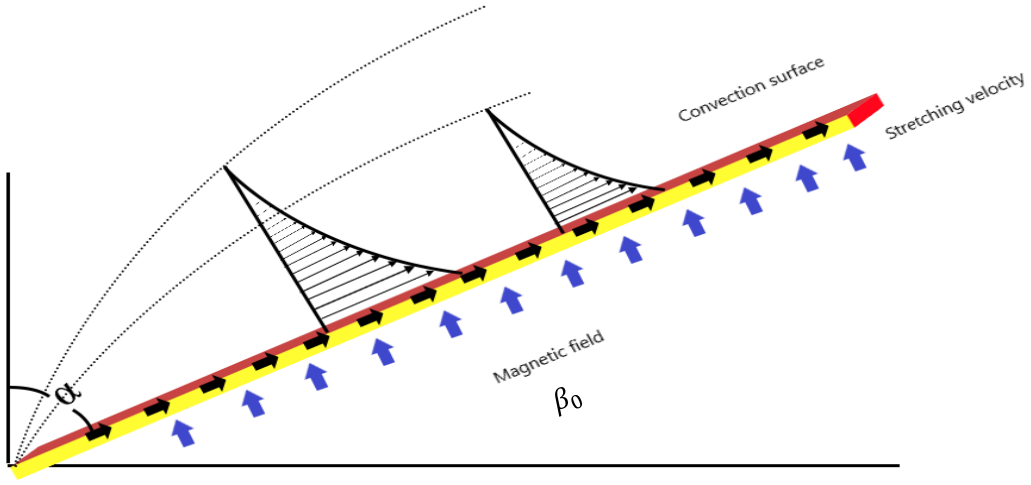

Figure 3.1: Geometry of a problem

$$\nabla.V = 0, \tag{3.1}$$

$$\rho\,(V.\nabla)V = div\tau - \sigma {B^2}_0\, V + J \times B, \tag{3.2}$$

$$\left(\rho C_p\right)(V.\nabla)T = \tau.(\nabla V) - divq, \tag{3.3}$$

Where τ can be written as;

$$\tau = -pI + \mu E_1. \tag{3.4}$$

Here E_1 is Rivlin-Ericksen tensor, which can be written as

$$E_1 = (\nabla V) + (\nabla V)^T, \tag{3.5}$$

$$J \times B = \left[-\delta {\beta_o}^2 u, 0,0\right]. \tag{3.6}$$

The respective velocity and temperature fields will be:

$$V = [u(x,y), v(x,y), 0], T = T(x,y), \tag{3.7}$$

$$\nabla V = \begin{bmatrix} u_x & u_y & 0 \\ v_x & v_y & 0 \\ 0 & 0 & 0 \end{bmatrix}, (\nabla V)^T = \begin{bmatrix} u_x & v_x & 0 \\ u_y & v_y & 0 \\ 0 & 0 & 0 \end{bmatrix}. \tag{3.8}$$

Using equation(3.8) in(3.5) we get

$$E_1 = \begin{bmatrix} 2u_x & u_y + v_x & 0 \\ v_x + u_y & 2v_y & 0 \\ 0 & 0 & 0 \end{bmatrix}. \tag{3.9}$$

Putting equation (3.9) in (3.4)

$$\tau = \begin{bmatrix} -p + 2\mu u_x & \mu(u_y + v_x) & 0 \\ \mu(v_x + u_y) & -p + 2\mu v_y & 0 \\ 0 & 0 & -p \end{bmatrix}. \tag{3.10}$$

Components of equation (3.10),

$$\left.\begin{aligned}&\tau_{xx} = -p + 2\mu u_x,\ \tau_{xy} = \tau_{yx} = \mu(v_x + u_y),\\&\tau_{xz} = \tau_{zx} = \tau_{yz} = \tau_{zy} = 0,\\&\tau_{yy} = -p + 2\mu v_y, \tau_{zz} = -p.\end{aligned}\right\} \quad (3.11)$$

Putting equation (3.11) in (3.2),

$$\left.\begin{aligned}&\rho(uu_x + vu_y) = -\frac{\partial p}{\partial x} + \mu\nabla^2 u - \sigma {B_o}^2 u + g\beta(T - T_\infty)\cos\alpha,\\&\rho(uv_x + vv_y) = -\frac{\partial p}{\partial x} + \mu\nabla^2 v - \sigma {B_o}^2 v + g\beta(T - T_\infty)\cos\alpha,\end{aligned}\right\} \quad (3.12)$$

In this case, $\cos\alpha$ is due to boundary layer flow caused by the inclined stretching sheet.

Now, using equation (3.3)

$$q = -k[T_x, T_{y,}0], \quad (3.13)$$

$$\rho C_p(uT_x + T_y) = k\nabla^2 T + \mu(\nabla T)^2, \quad (3.14)$$

$$\rho C_p\left(u\frac{\partial T}{\partial x} + \frac{\partial T}{\partial y}\right) = k\left(\frac{\partial^2 T}{\partial x^2}\right) + \mu\left(\frac{\partial u}{\partial y}\right)^2. \quad (3.15)$$

The boundary condition for equations are:

$$u = u_w(x) = cx\ , v = 0, T = T_w(x) = T_\infty + ax^2 \quad \text{at} \quad y \to 0$$

$$u \to 0, T \to 0 \quad \text{at} \quad y \to \infty$$

Here the Temperature and Velocity of the stretching boundary are T_w and u_w, respectively.

To convert PDE's into corresponding ODE's using the following transformation:

$$\eta = \left(\frac{c}{\nu}\right)^{\frac{1}{2}} y, u = cxf', v = -(c\nu)^{\frac{1}{2}} f, \theta = \frac{T - T_\infty}{T_w - T_\infty}, \tag{3.16}$$

By Utilizing equation (3.16) in

(3.12) and (3.14) we get governing equations:

$$f''' + ff' - f'^2 + \lambda\theta \cos\alpha - M^2 f'^2 = 0, \tag{3.17}$$

$$\frac{1}{Pr}\theta'' + f\theta' - 2f'\theta + Ecf''^2 = 0, \tag{3.18}$$

The dimensionless numbers appearing in the above equation are:

$$\left.\begin{aligned} M = \left(\frac{\sigma {B_o}^2}{\rho c}\right)^{\frac{1}{2}}, \lambda = \frac{Gr}{{Re_x}^2} = \frac{g\beta(T_w - T_\infty)}{{u_w}^2} = \frac{mga}{c^2}, \\ Pr = \frac{\nu}{\alpha^*}, Ec = \frac{{u_w}^2}{C_p(T_w - T_\infty)} = \frac{c^2}{C_p a}, \end{aligned}\right\} \tag{3.19}$$

Where M is the Magnetic parameter, λ is a thermal convective parameter, Pr and Ec are Prandtl and Eckert numbers, respectively. With boundary conditions:

$$f(0) = 0, f'(0) = 1, \theta(0) = 1, \tag{3.20}$$

$$f'(\infty) = 0, \theta(\infty) = 0. \tag{3.21}$$

While the Skin friction C_f and Nusselt number Nu_x be:

$$C_f = \frac{2\tau_w}{\rho u^2{}_w}, \qquad Nu_x = \frac{xq_w}{k(T_w - T_\infty)}, \tag{3.22}$$

Where τ_w is shear stress, k is thermal conductivity, and q_w is heat flux.

Using similarity (3.16) in (3.22), we have:

$$Re_x{}^{1/2}\, C_f = f''(0), \qquad Re_x{}^{-1/2}\, Nu_x = -\theta'(0). \tag{3.23}$$

3.2 Irreversibility Analysis:

The entropy generation rate per unit volume in the presence of a magnetic field is given by:

$$S_{gen}{}''' = \frac{k}{T^2}(\nabla T)^2 + \frac{\mu}{T}\,\Phi + \frac{1}{T}[(J - QV)\, \times (E + V \times B)] \tag{3.24}$$

Where Φ is viscous dissipation, J is current density and ∇ is the operator.

Using equation (3.15) in (3.24):

$$S_{gen}{}''' = \frac{k}{T^2}\left(\frac{\partial T}{\partial y}\right)^2 + \frac{\mu}{T}\left(\frac{\partial u}{\partial y}\right)^2 + \frac{1}{T}\left(\sigma B_o{}^2 u^2\right), \tag{3.25}$$

Now using (3.16) in (3.25), we have:

$$Ns = \frac{S_{gen}{}'''}{S_o{}'''} = \frac{\theta'^2}{(\theta + \Omega)^2} + \frac{Ec\,\mathrm{Pr}\, f''^2}{(\theta + \Omega)} + \frac{M\, Ec\,\mathrm{Pr}\, f'^2}{(\theta + \Omega)}, \tag{3.26}$$

Where $S_o''' = \frac{kc}{\nu}$ and $\Omega = \frac{T_\infty}{T_w - T_\infty}$ represent the Entropy and dimensionless Temperature.

$$Be = \frac{\frac{k}{T^2}\left(\frac{\partial T}{\partial y}\right)^2}{\frac{\mu}{T}\left(\frac{\partial u}{\partial y}\right)^2 + \frac{1}{T}\left(\sigma {B_o}^2 u^2\right)}, \tag{3.27}$$

Using (3.16)in (3.27), the Bejan number can be defined as:

$$Be = \frac{\theta'^2}{(\theta + \Omega)(M\, Ec \Pr f'^2 + Ec \Pr f''^2)}, \tag{3.28}$$

3.3 Numerical Methodology:

Using the shooting technique and Runge-Kutta method, the ordinary differential equations (3.17) and (3.18) with their corresponding boundary conditions (3.20) and (3.21) can be solved. The system (3.17), (3.18) be converted into a first order initial value problem in order to be solved. Thus, we take:

$f = t(1),$ $\theta = t(4),$

$f' = t(2),$ $\theta' = t(5),$

$f'' = t(3),$ $\theta'' = tt2,$

$f''' = tt1,$

Equation (3.17) $\Rightarrow tt1 = -t(1)t(3) + t(2)^2 - \lambda t(4)cos(\alpha) + M^2 t(2);$
Equation (3.18) $\Rightarrow tt2 = Pr(-t(1)t(5) + 2t(2)t(4) - Ec\ t(3)^2);$

$$\Rightarrow \begin{bmatrix} f' \\ f'' \\ f''' \\ \theta' \\ \theta'' \end{bmatrix} = \begin{bmatrix} t(2) \\ t(3) \\ tt1 \\ t(5) \\ tt2 \end{bmatrix} = \begin{bmatrix} t(2) \\ t(3) \\ -t(1)t(3) + t(2)^2 - \lambda t(4)cos(\alpha) + M^2 t(2) \\ t(5) \\ Pr * (-t(1)t(5) + 2t(2)t(4) - Ec\ t(3)^2) \end{bmatrix}$$

Here are the initial conditions:

$$t(1)(0) = 0\ , t(2)(0) = 1\ , t(4)(0) = 1,$$

$$t(2)(\infty) = 0, t(4)(\infty) = 0,$$

3.4 Result and Discussion:

By adopting a similarity transformation, the governing boundary layer equations are converted into standard differential equations, which are then resolved using the Runge-Kutta method. After the problem has been solved, it is evident that several new parameters, including the magnetic field parameter M, the entropy generation number Ns, the Eckert number Ec, the Prandtl number Pr, the buoyancy parameter, and the dimensionless temperature parameter, have been added. Through the use of graphs, this section will discuss the effects of these parameters on the Velocity and temperature profile.

The impact of M (the magnetic field) on the velocity profile is shown in Figure 3.2 (a). The transverse magnetic field, which produces the Lorentz force (a retarding force) and lowers the fluid Velocity, causes the velocity profile to decrease as the magnetic field M increases. As buoyancy forces increase, the velocity profile rises—figure 3.2 (b).

Figure 3.3 (a) shows the effect of Prandtl number Pr on fluid Temperature, concluding that large Prandtl number values decrease temperature velocity. They are pictured in Figure 3.3 (b). The buoyancy parameter causes the fluid's Temperature to decrease. The retarding force system creates the presence of a magnetic field, increasing the fluid friction and causing an increase in temperature Figure 3.4.

An increase in Pr increases the temperature gradients in the boundary layer, which boosts the dimensionless entropy generations Ns. Figure 3.5 (a) clearly shows the results. By rewinding the second law of thermodynamics, Figure 3.5 (b) shows that Entropy will be minimum by reducing the magnetic field effect. In Figure 3.6 (a) increase in λ decreases Ns, and as we move away from the boundary layer, it becomes zero. Results in Figure 3.6 (b) illustrate the increase of entropy generation Ns as the increase in Eckert number Ec. Here we can observe the second law of thermodynamics, which minimizes the entropy rate per unit volume. This effect is only observed on the surface of the stretching sheet and does not affect fluid flow. Increase in Ω, and the dimensionless temperature parameter increases Ns as in Figure 3.7. This demonstrates that Ns becomes zero as they move away from the boundary layer.

Figure 3.8 (a) signifies the effects of Magnetic field M on Bejan number Be, which demonstrates increase in Be in an increase of M. From Figure,rise in Magnetic field yields viscosity and magnetic irreversibility to control temperature irreversibility of stretching sheet. The surface viscosity and magnetic irreversibility entirely regulate the thermal irreversibility for $M > 2$. Although, distance from stretching sheet outcome alters. From the plot Figure 3.8 (b), it is evident that magnetic field and fluid friction are significant factors in the formation of overall Entropy, as Be decreases in the Pr increase for a fixed value of η. Additionally, it can be seen that the Bejan number Be becomes almost zero, close to the stretched sheet's surface. Figure 3.9 (a) demonstrates the effect of λ on Be, which increases with an increase in the value of λ. For small values of Ω, the heat transfer effect dominates far from the surface of the stretching sheet, which is observed in Figure 3.9 (b) the increase in value of Ω decreases Be. Figure 3.10 illustrates how the rise in Ec reduces the impact of Bejan number Be. Although the progress of heat transfer in entropy generation is evident far from the surface of the stretching sheet, the effect of magnetic and viscous irreversibility controls the conductive irreversibility.

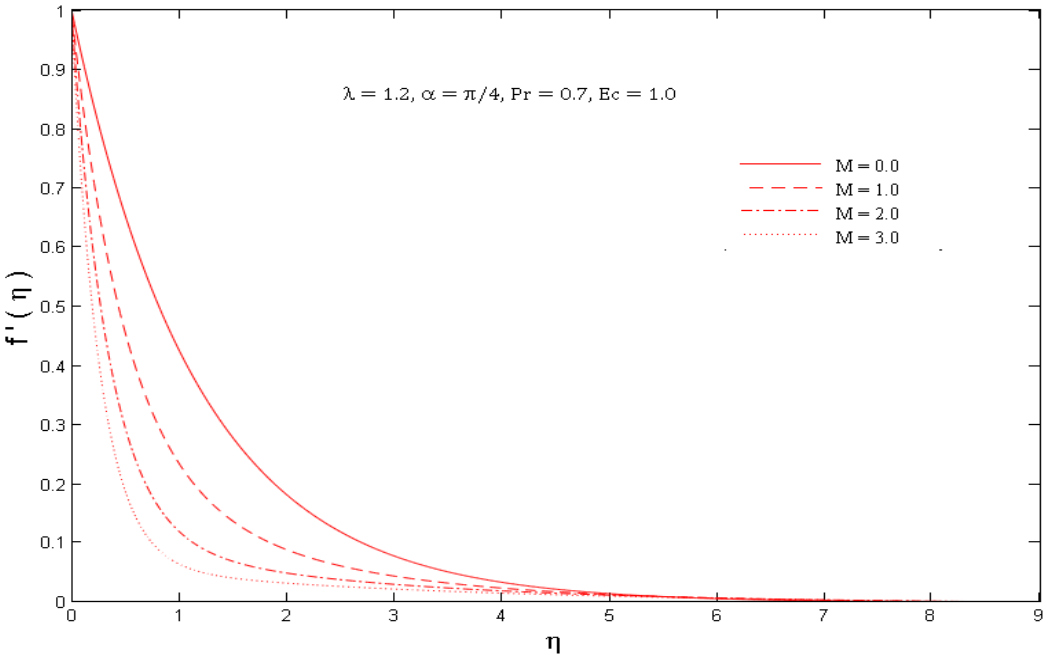

(a)

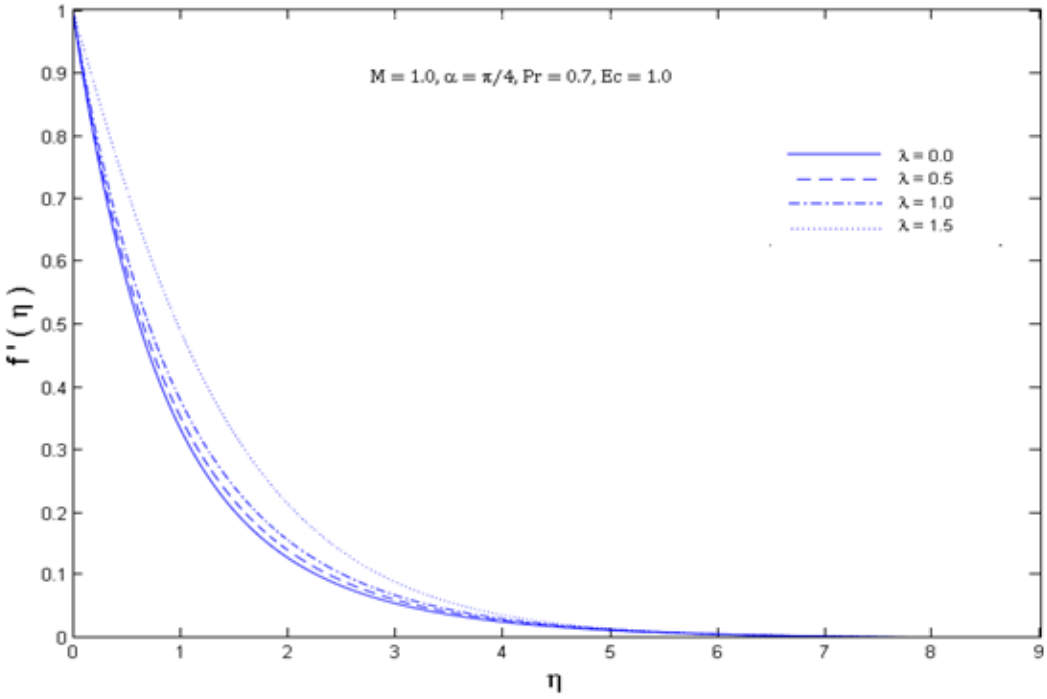

(b)

Figure 3.2: Variations in the velocity profile with respect to M and λ

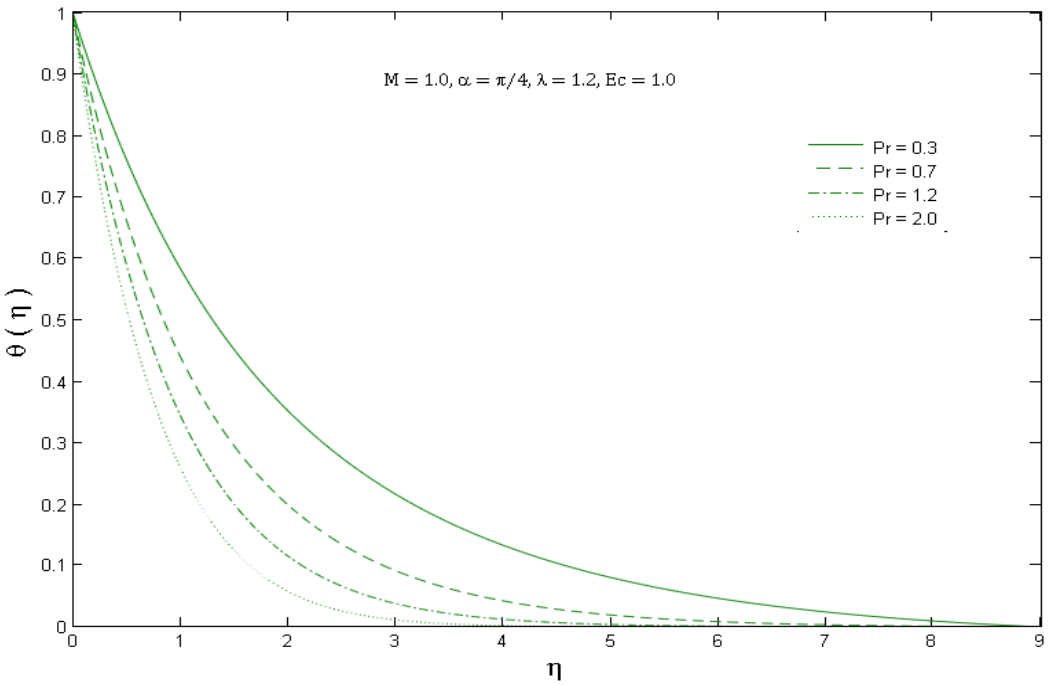

(a)

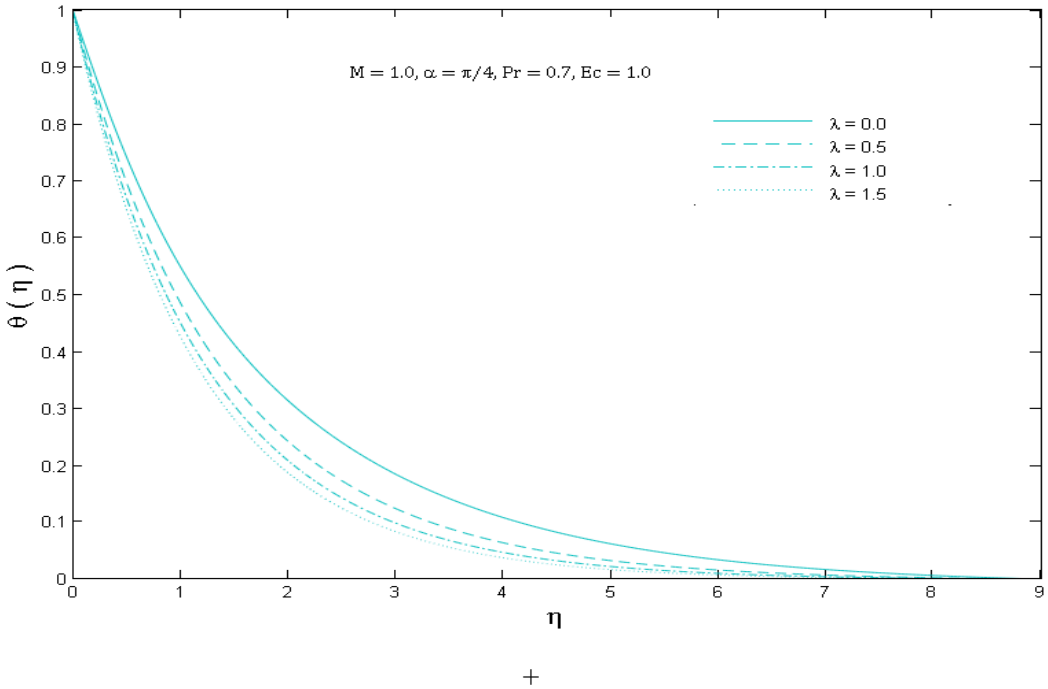

Figure 3.3: Variations in the temperature profile with respect to Pr and λ.

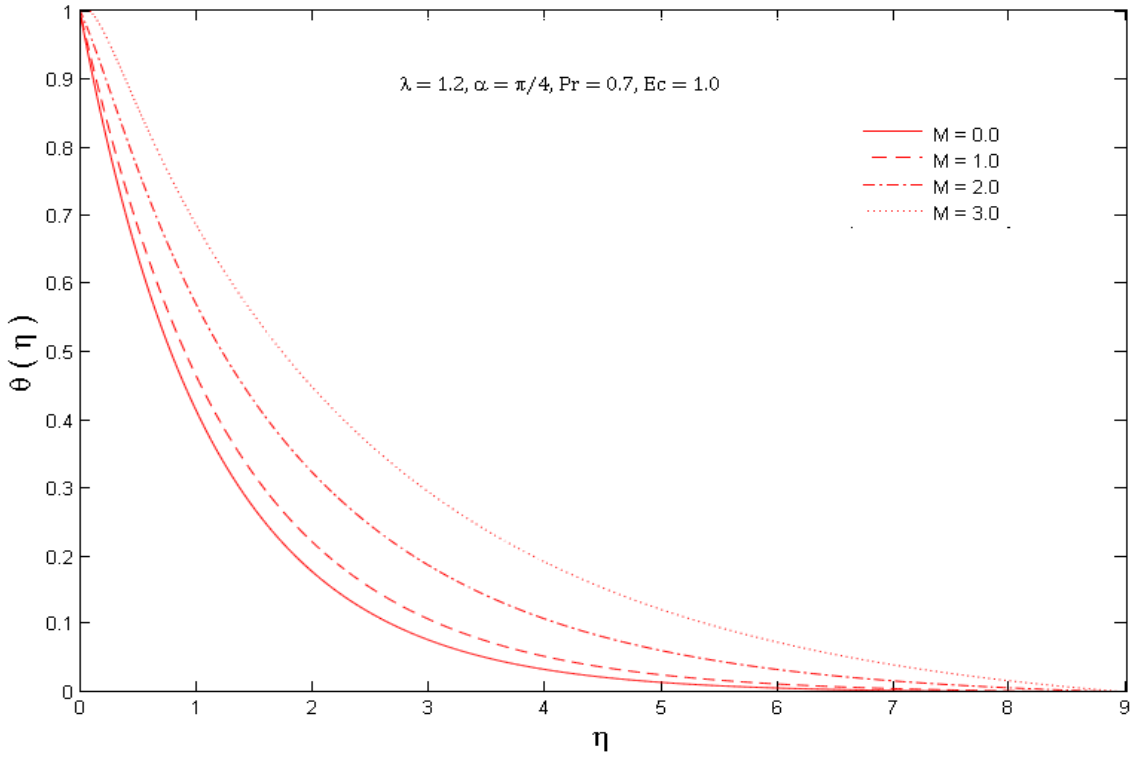

Figure 3.4: Variations in the temperature profile with respect to M.

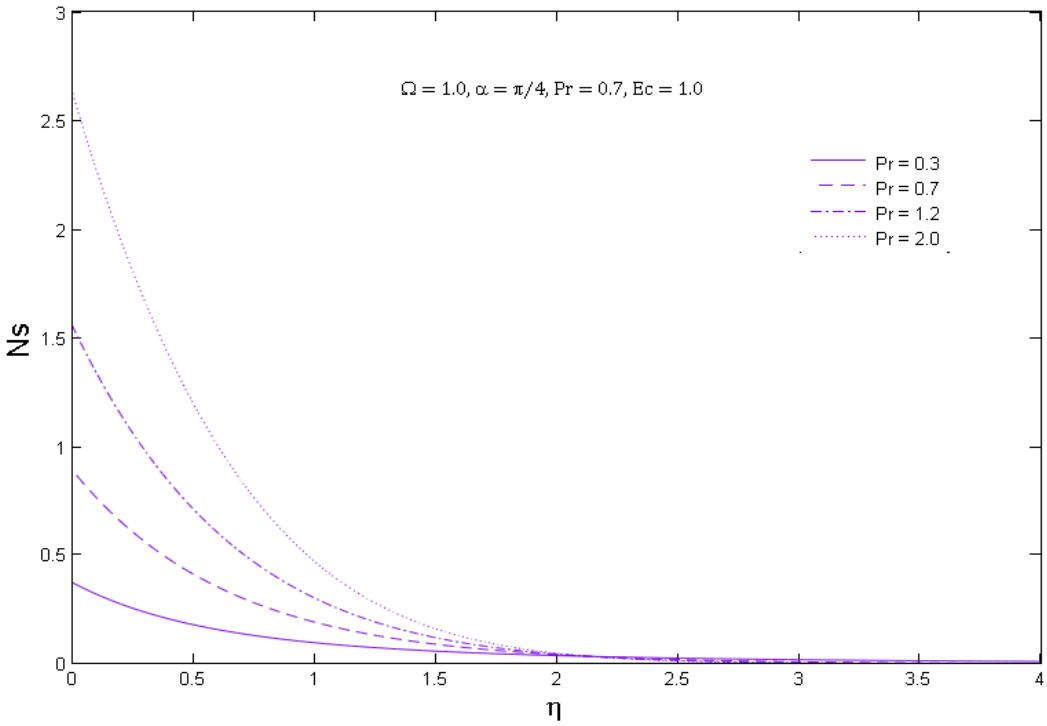

(a)

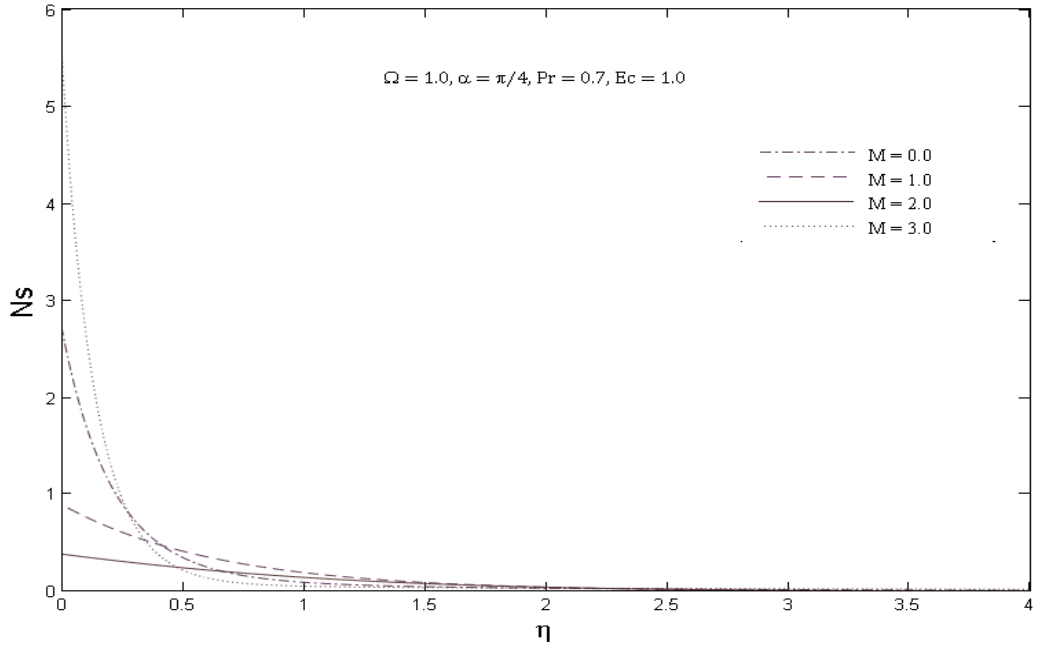

(b)

Figure 3.5: Variations in the entropy generation with respect to Pr and M.

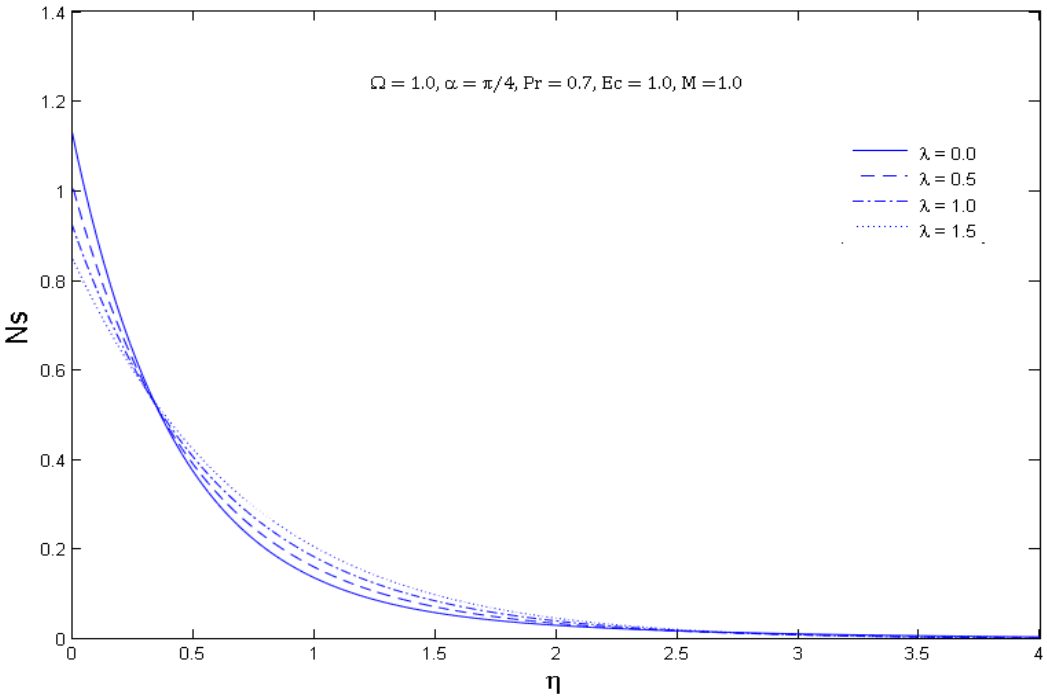

(a)

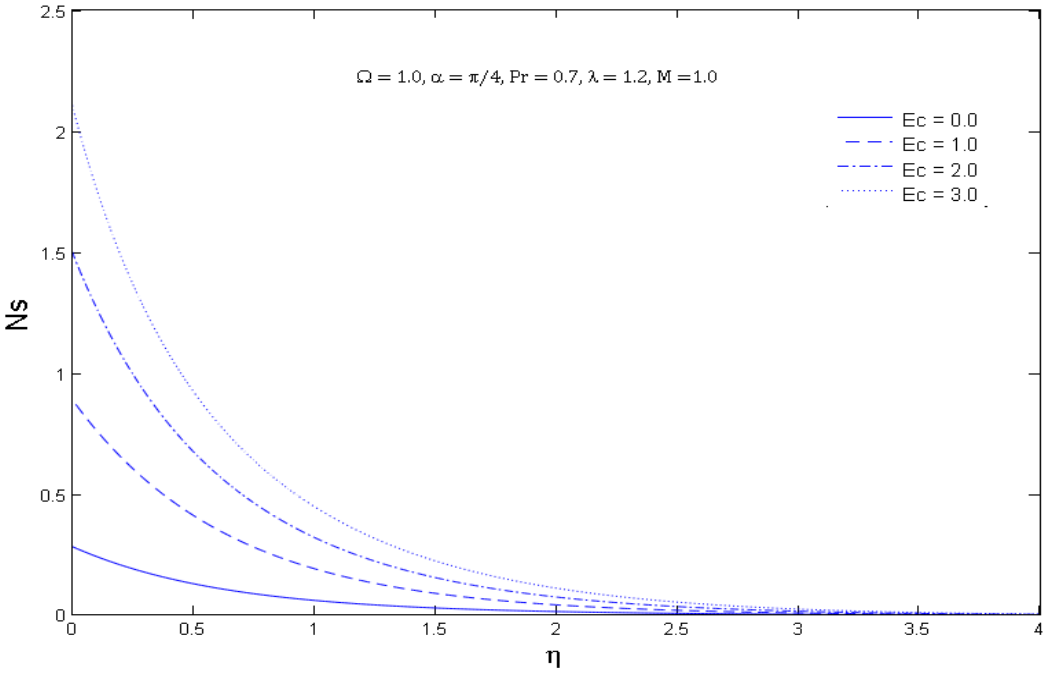

(b)

Figure 3.6: Variations in the entropy generation with respect to λ and Ec.

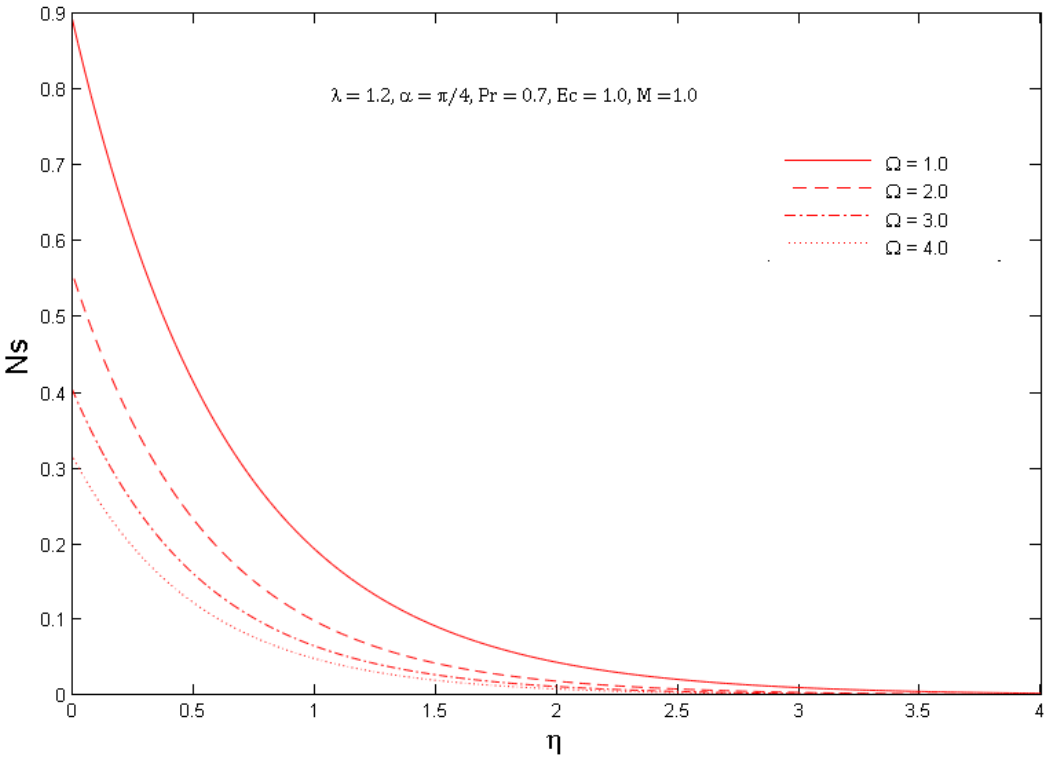

(c)

Figure 3.7: Variations in the entropy generation with respect to Ω.

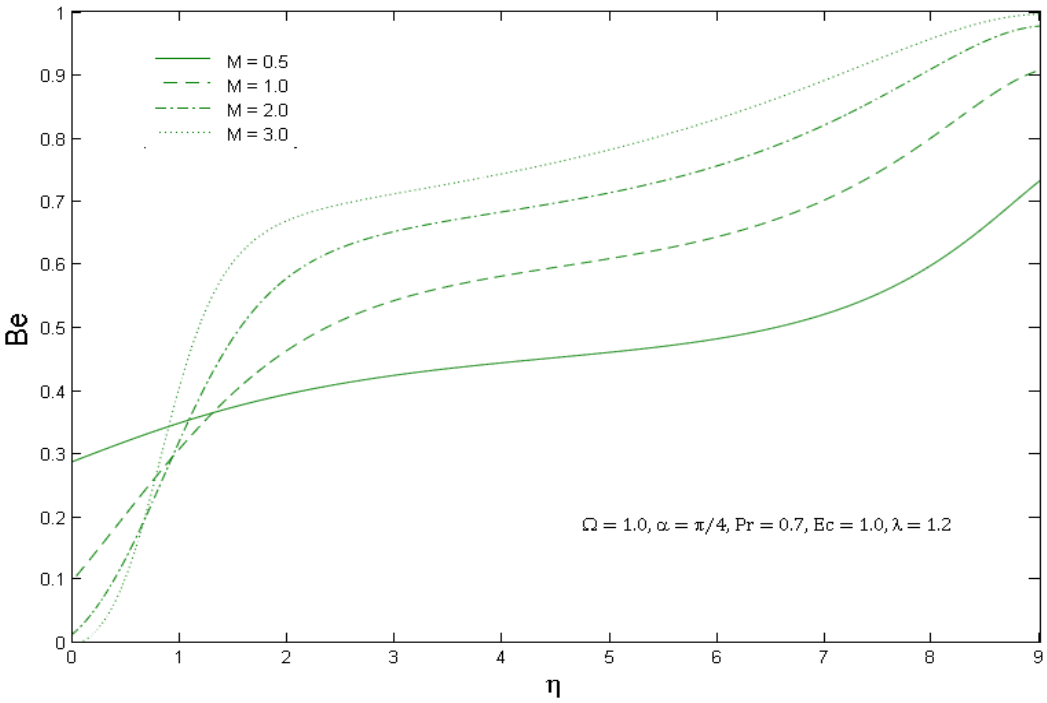

(a)

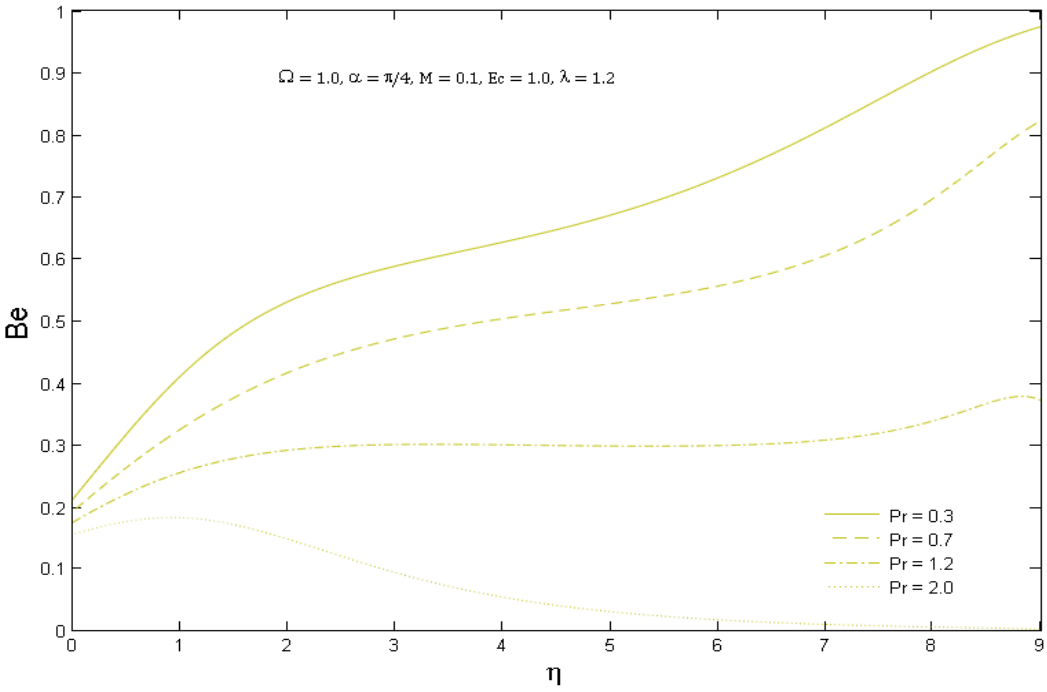

(b)

Figure 3.8: Variations in the Bejan number with respect to Pr and M.

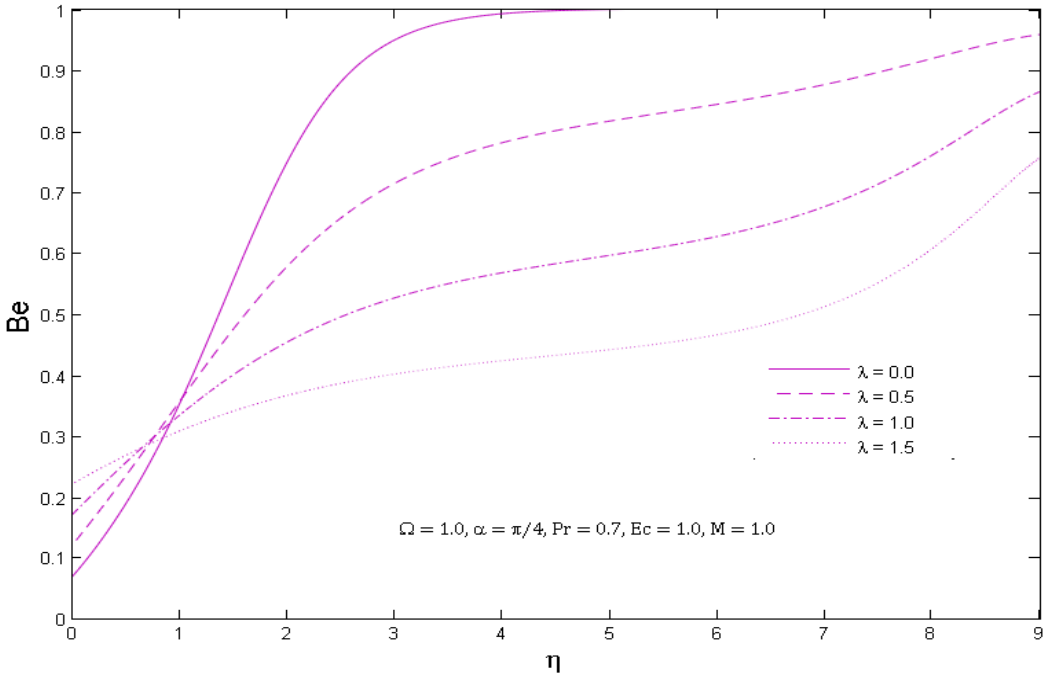

(a)

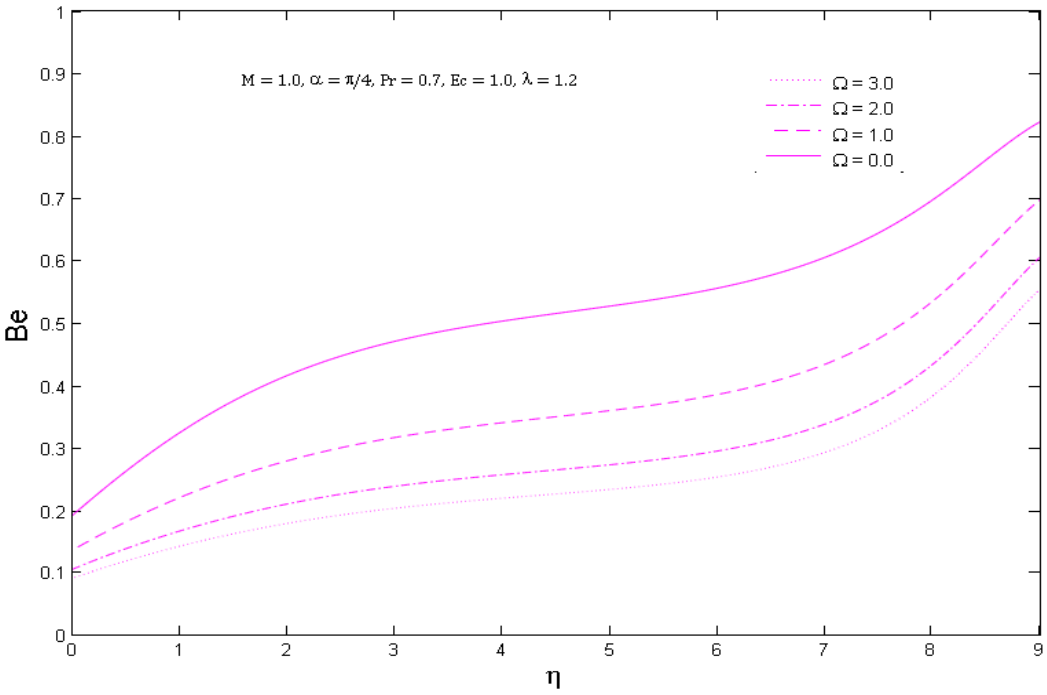

(b)

Figure 3.9: Variations in the Bejan number with respect to λ and Ω.

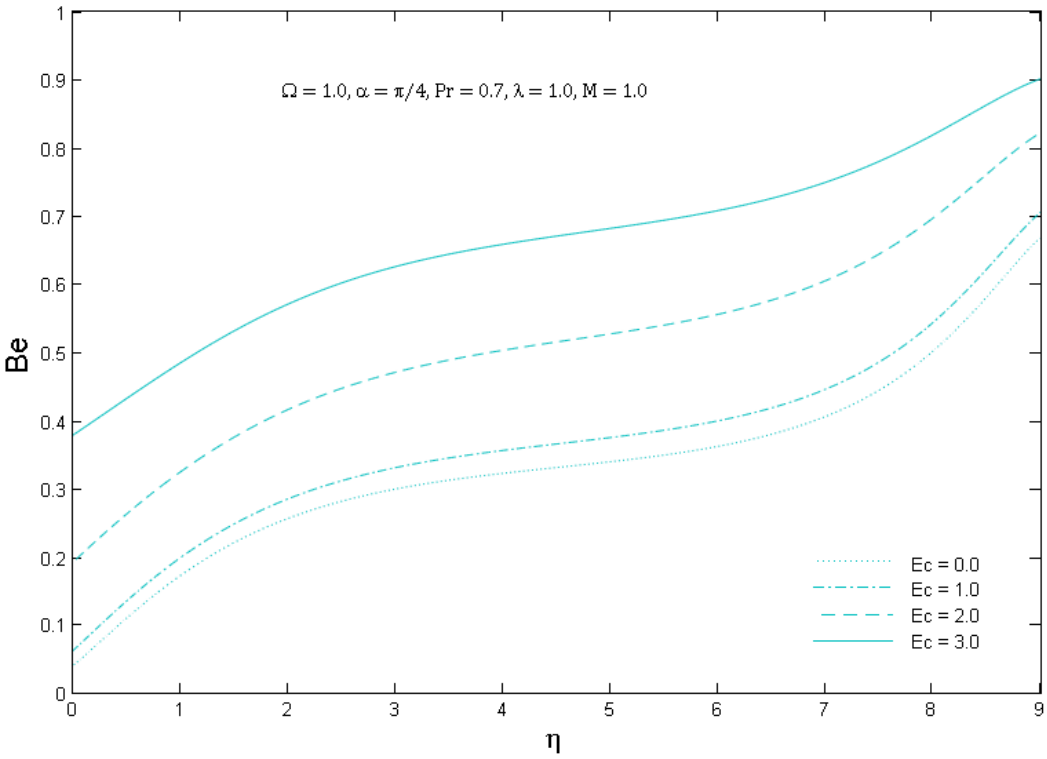

(c)

Figure 3.10: Variations in the Bejan number with respect to Ec.

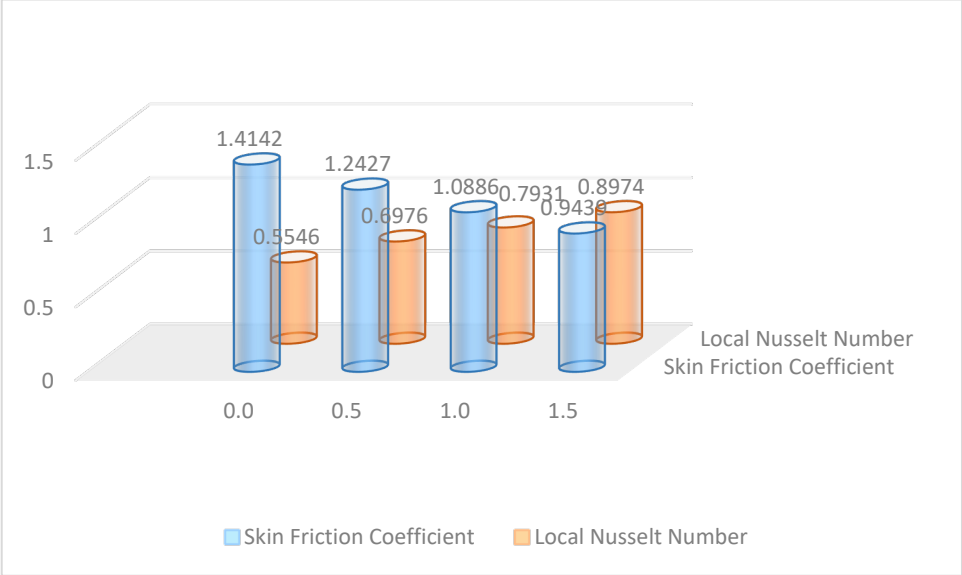

Figure 3.11: Outcomes of λ on skin friction coefficient and local Nusselt number.

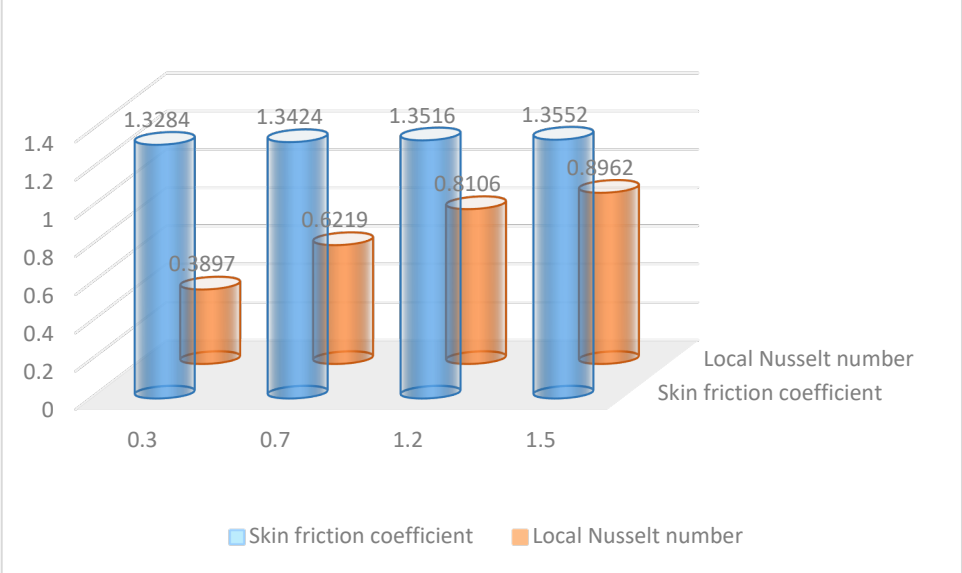

Figure 3.12: Outcome of Pr on skin friction coefficient and local Nusselt number.

CHAPTER 4

ENTROPY ANALYSIS DUE TO FREE CONVECTION FLOW ALONG VERTICAL SURFACE

With the addition of particular effects and limitations, this chapter expands on the previous chapter—the interaction between a nanofluid particle's form, thermal radiation, and velocity slip conditions. Additionally, a standard magnetic field $\boldsymbol{B_o}$ is applied to the stretching sheet. Additionally, it is presumed that the nanofluid is made of water and contains nanoparticles in various shapes. A similarity transformation will be used to further rearrange the mathematical modeling with new effects before converting it into an ordinary differential equation. Finally, use MATLAB to illustrate the outcome graphically.

4.1 Mathematical modeling:

Consider a steady two-dimensional flow over a stretching sheet. With viscous nanofluid dissipation effect along a vertical surface. $u = U_w(x) = cx + L\frac{\partial u}{\partial y}$ (Where c is a constant) is the Velocity slip condition. The governing equations are:

$$\frac{\partial u}{\partial x} + \frac{\partial v}{\partial y} = 0, \tag{4.1}$$

$$\rho_{nf}\left(\frac{\partial u}{\partial x} + \frac{\partial v}{\partial y}\right) = \mu_{nf}\frac{\partial^2 u}{\partial y^2} - \sigma_{nf}{B_o}^2 u + g(\rho\beta)_{nf}(T - T_\infty), \tag{4.2}$$

$$(\rho C_p)_{nf}\left(u\frac{\partial T}{\partial x} + v\frac{\partial T}{\partial y}\right) = \kappa_{nf}\frac{\partial^2 T}{\partial y^2} + \mu_{nf}\left(\frac{\partial u}{\partial y}\right)^2 - \frac{\partial q_r}{\partial y}, \tag{4.3}$$

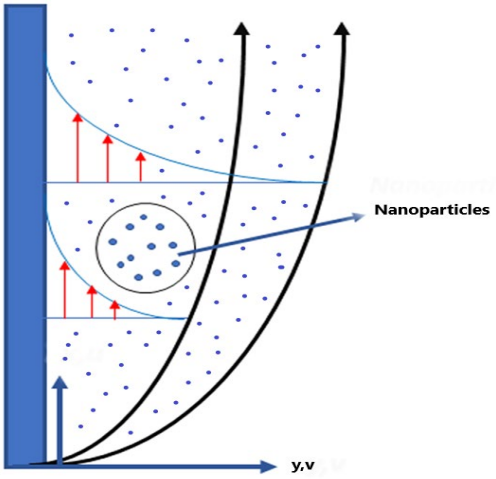

Figure 4.1: Geometry

Where $\frac{\partial q_r}{\partial y}$ is radiation heat flux, by using Rosseland approximation:

$$q_r = -\left(\frac{4\breve{\sigma}}{3\breve{K}}\right)\left(\frac{\partial T^4}{\partial y}\right), \tag{4.4}$$

$$\text{Where } T^4 \cong 4T^3{}_\infty T - 3\acute{T}^4{}_\infty, \tag{4.5}$$

Where here, $\breve{K}$ is absorption co-efficient and $\breve{\sigma}$ Stefan Boltzmann constant.

Now by using the value of T^4 in q_r we get,

$$q_r = -\left(\frac{16\breve{\sigma}\ T^3{}_\infty}{3\breve{K}}\right)\left(\frac{\partial T}{\partial y}\right), \tag{4.6}$$

$$(\rho C_p)_{nf}\left(u\frac{\partial T}{\partial x} + v\frac{\partial T}{\partial y}\right) = \kappa_{nf}\frac{\partial^2 T}{\partial y^2} + \mu_{nf}\left(\frac{\partial u}{\partial y}\right)^2 + \left(\frac{16\sigma\ T^3{}_\infty}{3K}\right)\left(\frac{\partial T}{\partial y}\right), \tag{4.7}$$

So respective boundary conditions will be,

$$\left.\begin{array}{ll} u = U_w(x) = cx + L\dfrac{\partial u}{\partial y} & at\ y = 0 \\ v = 0, T = T_w(x) = T_\infty + ax^2 & at\ y = 0 \\ u = 0, T = 0 & as\ y = \infty \end{array}\right\} \quad (4.8)$$

Physical Properties of Nanofluid particle can be define as:

$$\left.\begin{array}{l} \mu_{nf} = \dfrac{\mu_f}{(1-\phi)^{2.5}}, \\ \rho_{nf} = (1-\phi)\rho_f + \phi\rho_s, \\ \dfrac{\sigma_{nf}}{\sigma_f} = 1 + \dfrac{3\left(\frac{\sigma_s}{\sigma_f}-1\right)\phi}{\left(\frac{\sigma_s}{\sigma_f}+2\right)-\left(\frac{\sigma_s}{\sigma_f}-1\right)\phi}, \\ B_{nf} = (1-\phi)B_f + \phi B_s, \\ (\rho C_p)_{nf} = (1-\phi)\left(\rho C_p\right)_f + \phi(\rho C_p)_s, \end{array}\right\} \quad (4.9)$$

The Brownian movement has major effects on thermal conductivity. According to Koo and Kleinstreuer [30, 31], effective thermal conductivity comprises two parts: static and Brownian motion. The Brownian motion has a significant consequence on thermal conductivity.

$$k_{nf} = k_{static} + k_{Brownian},$$

Where

$$\frac{k_{static}}{k_f} = 1 + \frac{3\left(\frac{k_p}{k_f}-1\right)\phi}{\left(\frac{k_p}{k_f}+2\right)-\left(\frac{k_p}{k_f}-1\right)\phi}, \quad (4.10)$$

$$k_{Brownian} = 5 \times 10^4 \left(\rho C_p\right)_f \beta \, \phi \sqrt{\frac{k_b T^*}{d_p \rho_p}} \, g(T^*, \phi). \tag{4.11}$$

Later KKL value was updated by [30] using,

$$R_f = \frac{d_p}{k_p} = \frac{d_p}{k_{p.eff}}, \tag{4.12}$$

$$\begin{aligned} G\left(T^*, \phi, d_p\right) = (\dot{b_1} + \dot{b_2} \ \ln(d_p) \\ + \dot{b_3} \ln(\phi) + \dot{b_4} \ln(\phi) \ln(d_p) \\ + \dot{b_5} \ \ln(d_p)^2 \ln(T^*) + (\dot{b_6} \dot{b_7} \ln(d_p) + \dot{a_8} \ln(\phi) \\ + \dot{b_9} \ln(d_p) \ln(\phi) + \dot{b_{10}} \ \ln(d_p)^2. \end{aligned} \tag{4.13}$$

Finally, KKL correlation can be written as:

$$k_{Brownian} = 5 \times 10^4 \phi \left(\rho C_p\right)_f \sqrt{\frac{k_b T^*}{\rho_p d_p}} \, G\left(T^*, \phi \, , d_p\right), \tag{4.14}$$

$$\mu_{nf} = \mu_{static} + \mu_{Brownian} = \mu_{static} + \frac{k_{Brownian}}{k_f} \times \frac{\mu_f}{Pr_f}. \tag{4.15}$$

According to Hamilton and Crosser (1962) [38], the shape-dependent effects:

$$\frac{k_{nf}}{k_f} = \frac{-\left(k_f - k_p\right) m\phi + \left(k_p - k_f\right)\phi + mk_f + k_p + k_f}{mk_f + \left(k_f - k_p\right)\phi + k_f + k_p}. \tag{4.16}$$

Table 4.1 Thermal properties of CuO and water [30, 31]

Physical properties	**Pure Water**	$\boldsymbol{CuO}$
$\rho(kg/m^3)$	997.1	6500
$C_p(J/kgK)$	4179	540
$K(W/mK)$	0.613	18
dp	-	29
$\sigma\ (\Omega.m)^{-1}$	0.05	10^{-10}

Table 4.2 Coefficient values of CuO-water nanofluids

Coefficient	$\boldsymbol{CuO}$**-water values**
$\dot{b_1}$	-26.5933108
$\dot{b_2}$	-0.403818333
$\dot{b_3}$	-33.3516805
$\dot{b_4}$	-1.915825591
$\dot{b_5}$	6.421858E-2
$\dot{b_6}$	48.40336955
$\dot{b_7}$	-9.787756683
$\dot{b_8}$	190.245610009
$\dot{b_9}$	10.9285386565
$\dot{b_{10}}$	-0.72009983664

Table 4.3 Shape factors (m) parameter [38]

Shapes	**Platelet**	**Brick**	**Spherical**
m	5.7	3.7	3.0

Using the similarity variables as:

$$\eta = \left(\frac{c}{\nu_f}\right)^{1/2} y, \qquad u = cxf', \qquad \theta = \frac{T - T_\infty}{T_w - T_\infty}, \qquad v = -\left(c\nu_f\right)^{1/2} f, \tag{4.17}$$

Using similarity transformation in equation (4.17)

$$A_1 f''' + A_2\left[ff'' - f'^2\right] - A_3 M f' + A_2 A_4 \lambda\theta = 0, \tag{4.18}$$

$$\theta''[A_5 + Rd] + A_6 \Pr[f\theta' - 2f'\theta] + A_1 Ec \Pr f''^2 = 0 \tag{4.19}$$

With respective Parameters:

$$\left.\begin{aligned} &A_1 = \frac{\mu_{nf}}{\mu_f}, A_2 = \frac{\rho_{nf}}{\rho_f}, A_3 = \frac{\sigma_{nf}}{\sigma_f}, A_4 = \frac{B_{nf}}{B_f}, A_5 = \frac{k_{nf}}{k_f}, \\ &A_6 = \frac{\left(\sigma C_p\right)_{nf}}{\left(\sigma C_p\right)_f}, \\ &Rd = \frac{16\sigma {T_\infty}^3}{3Kk_f}, M = \frac{\sigma_f {B_o}^2}{c\rho_f}, Pr = \frac{\nu_f\left(\rho C_p\right)_f}{k_f}, \\ &Ec = \frac{(cx)^2\rho_f}{\left(\rho C_p\right)_f (T_w - T_\infty)}, \end{aligned}\right\} \tag{4.20}$$

So boundary conditions will be:

$$\left.\begin{aligned} &f(0) = 0, f'(0) = 1 + \delta f''(0), \theta(0) = 1 \quad && at\ y = 0 \\ &f'(\eta) = 0, \theta(\eta) = 0 && as\ \eta = \infty \end{aligned}\right\} \tag{4.21}$$

Where $\delta = L\left(\frac{c}{\nu_f}\right)^{1/2}$.

While C_f and Nu_x are expressed as:

$$C_f = \frac{2\tau_w}{\rho_f {u_w}^2} = \frac{f''(0)}{(Re_x)^{1/2}(1-\phi)^{2.5}}, \tag{4.22}$$

$$Nu_x = \frac{xq_w}{k_f(T_w - T_\infty)} = \frac{-(A_5 + Rd)\theta'(0)}{(Re_x)^{-1/2}}. \tag{4.23}$$

Where $(Re_x)^2 = \frac{cx^2}{\nu_f}, q_w = -\left(k_{nf} + \frac{16\hat{\sigma}{T^3}_\infty}{3\hat{K}}\right)\left(\frac{\partial T}{\partial y}\right)_{y=0}$,

$\tau_w = -\mu_{nf}\left(\frac{\partial u}{\partial y}\right)_{y=0}$,

Local Reynolds number, shear stress, and heat flux, respectively

4.2 Irreversibility Analysis:

The entropy generation rate per unit volume in the presence of a magnetic field is given by:

$${S_{gen}}''' = \frac{k}{T^2}(\nabla T)^2 + \frac{\mu}{T}\,\Phi + \frac{1}{T}[(J - QV)\,\times (E + V \times B)]. \tag{4.24}$$

Where Φ is viscous dissipation, J is current density and ∇ is an operator.

Using the above equations:

$${S_{gen}}''' = \frac{k}{T^2}\left(1 + \frac{16\sigma {T_\infty}^3}{3K}\right)\left(\frac{\partial T}{\partial y}\right)^2 + \frac{\mu}{T}\left(\frac{\partial u}{\partial y}\right)^2 + \frac{1}{T}\left(\sigma {B_o}^2 u^2\right). \tag{4.25}$$

Now using similarity transformation above equation becomes:

$$Ns = \frac{\theta'^2}{(\theta+\Omega)^2}A_5(1+Rd) + \frac{Ec\,\Pr f''^2}{(\theta+\Omega)}A_1A_2 + \frac{M\,Ec\,\Pr f'^2}{(\theta+\Omega)}A_3. \quad (4.26)$$

Where $S_o''' = \frac{k_f c}{\nu_f}$ and $\Omega = \frac{T_\infty}{T_w - T_\infty}$ represent the Entropy and dimensionless Temperature.

Using the above and similarity transformation Bejan number can be defined as:

$$Be = \frac{A_5\theta'^2(1+Rd)}{A_5\theta'^2(1+Rd) + (\theta+\Omega)(Ec\,\Pr)(A_1A_2f''^2 + MA_3f'^2)}. \quad (4.27)$$

4.3 Numerical Methodology:

In order to solve the ordinary differential equations (4.17) and (4.18) with respective boundary conditions (4.20) by using the shooting technique along with the Runge-Kutta method. Solve the first step is to transform the systems (4.17) and (4.18) into first-order initial value problems, so we take:

$f = t(1),$ $\theta = t(4),$

$f' = t(2),$ $\theta' = t(5),$

$f'' = t(3),$ $\theta'' = tt2,$

$f''' = tt1,$

Eq(4.17) $\Rightarrow tt1 = (1/A1) - A2y(1)y(3) - y(2)^2 - \lambda A2A4y(4) + A3My(2);$
Eq(4.18) $\Rightarrow tt2 = (A5 + Rd)(-A6\Pr(y(1)y(5) - 2y(2)y(4)) - A1EcPry(3)^2);$

$$\Rightarrow \begin{bmatrix} f' \\ f'' \\ f''' \\ \theta' \\ \theta'' \end{bmatrix} = \begin{bmatrix} t(2) \\ t(3) \\ tt1 \\ t(5) \\ tt2 \end{bmatrix} = \begin{bmatrix} t(2) \\ t(3) \\ (1/A1)\ -A2t(1)t(3) - t(2)^2 - \lambda A2A4t(4) + A3Mt(2) \\ t(5) \\ (A5 + Rd)(-A6\Pr\,(t(1)t(5) - 2t(2)t(4)) - A1EcPrt(3)^2) \end{bmatrix}$$

Here, the initial conditions are:

$$t(1)(0) = 0, t(2)(0) = 1 + \delta t(3)(0), t(4)(0) = 1,$$

$$t(2)(\infty) = 0, t(4)(\infty) = 0,$$

4.4 Result and Discussion:

In this preceding, the previous results are adding nanofluid particles, including thermal radiations and magnetic fields. The governing partial differential equation transforms to ordinary differential equations using similarity transformation, which are solved numerically using MATLAB. New parameters are introduced, which includes Prandtl number Pr, Reynold number Re_x, Nusselt number Ns, magnetic field parameter M, convective parameter λ, Eckert number Ec, Bejan number Be, Grashof number Gr_x and velocity, temperature parameters Ω. In addition behavior of nanoparticles is also plotted. The effect of Cu/water nanofluid for different values of Pr, M, Ec, λ, and Ω also be seen. For shape parameter m, used values are $m = 5.7, m = 3.7, and\ m = 3.0$ for platelet, brick, and spherical.

Figure 4.2-4.4 illustrate the velocity profile with changing M,λ, and Pr values which are magnetic field, convective parameter, and Prandtl number, respectively, in the presence of shape effect m. It is observed that in Figure 4.2, the changing values of λ, the Velocity of nanofluid is increasing by increasing λ. Physically it is also anticipated that an increase in buoyancy/mixed convection enhances the velocity profile. The velocity profile always has a more significant effect compared to values of air and water, $Pr =$

0.71 and $Pr = 7.0$, respectively. So it is concluded graphically in Figure 4.3 that there is an increasing effect in the velocity field with different values of Pr between $0.71 - 7.0$. A decrease in velocity profile has been observed in Fig.4.4 as the magnetic field generates a drag called Lorentz (retarding) force which retards the fluid's motion with different $M = 1.0,2.0,3.0$. The magnetic parameter has a massive effect on nanofluid particles containing water as base fluid. It is also noticed that the performance of the platelet is better than brick and spherical on the velocity profile.

Dimensionless convection force parameter λ is a ratio of buoyancy forces to inertia force inside the boundary layer for free/forced convection. When $\lambda \to 0$, it states that forced convection is free for larger values of λ. Figure 4.5 depicts that the temperature profile is getting low (decrease) for larger values of λ, so the boundary layer changes free to forced convection under the circumstances. The effects of retarding (Lorentz) force can be seen in Figure 4.6, which boosts the nanofluid friction and this rise the temperature profile. Prandtl number has low thermal diffusion, which decreases the temperature field in nanofluid Figure 4.7 proves this phenomenon. On temperature distribution, the platelet performance is better than brick and spherical.

Ec, Eckert number is here dimensionless parameter which affects the entropy generation number Ns with increasing factor. It Figure 4.8 satisfies the second law of thermodynamics. Figure 4.9 shows the comparison of Ns with different values of λ along with the shape effect of platelet, bricks, and spherical, which shows a decrease in the ratio of increasing values of convective parameter λ. According to second law of thermodynamics, by reducing magnetic force there is minimization of entropy generation and hence graphically it is shown in Figure 4.10. In nanofluid, water as base fluid and nanoparticles in the shape of platelet, bricks, and spherical when we increase the Ω temperature dimensionless parameter clear view of an increase in Entropy is seen Figure 4.11. Although if you move away from the boundary layer, the irreversibility becomes zero. The temperature factor in the Prandtl number affects the Entropy directly. This investigation is proved in Figure 4.12 as an increase of Pr increase the Ns.

Entropy generation involvement in the heat transfer process is notable as far away from the stretching sheet compared to the surface of the stretching sheet. Figure 4.13

illustrate the decreasing effect on Bejan number Be of increasing Eckert number Ec. Rules apply to thermal irreversibility for $M > 2$; however, magnetic and viscosity irreversibility effects are reversed if we move away from the stretching sheet. As Figure 4.14 shows the decreasing effect of $the\ M$ magnetic field on the Bejan number. Magnetic field and fluid friction always play a vital role in entropy generation representation as in Figure 4.15 for values of η, the Bejan number Be decreases as an increase in Pr Prandtl number. Bejan number Be is also getting zero, close to the stretching sheet surface. Following the discussion, Figure 4.16 shows the descending effect in Be Bejan number with positive dimensionless temperature parameter Ω. It is also observed that the platelet nanoparticles have a higher rate of heat transfer than brick and spherical ones.

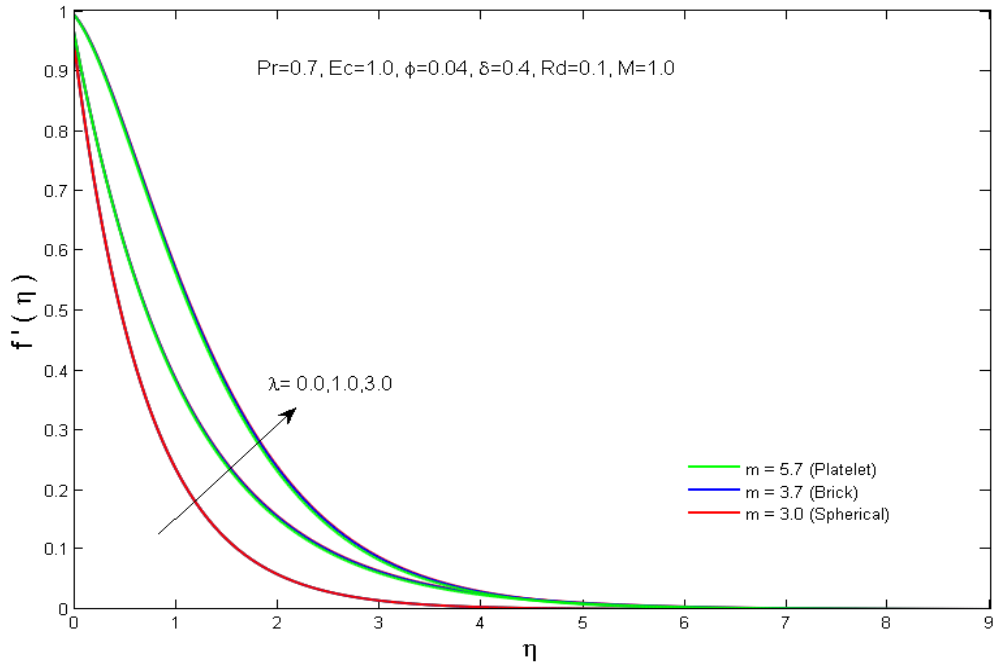

Figure 4.2: Variations in the Velocity with respect to λ.

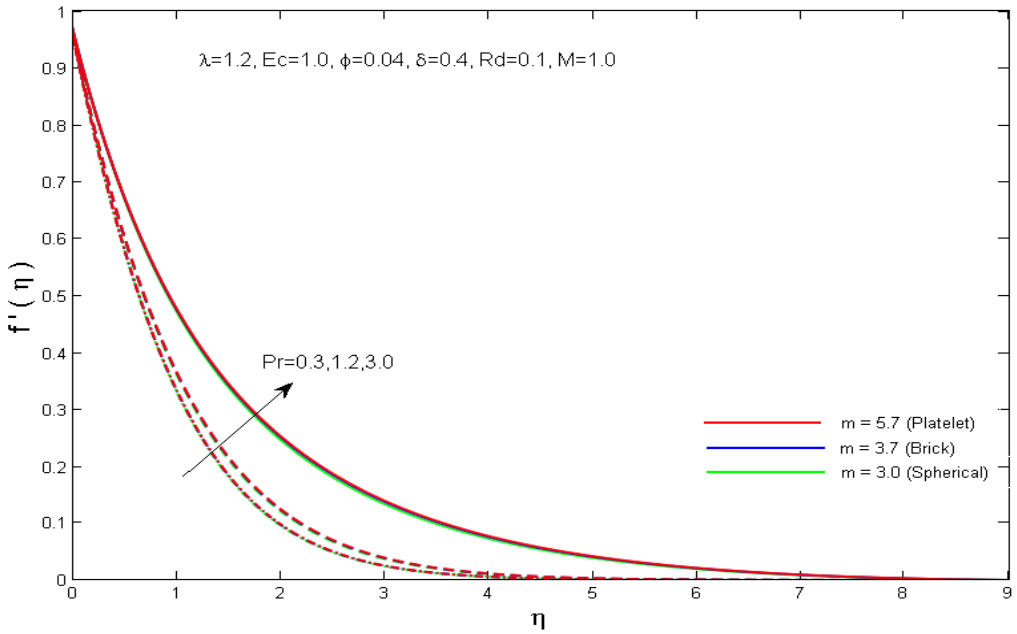

Figure 4.3: Variations in the Velocity with respect to Pr.

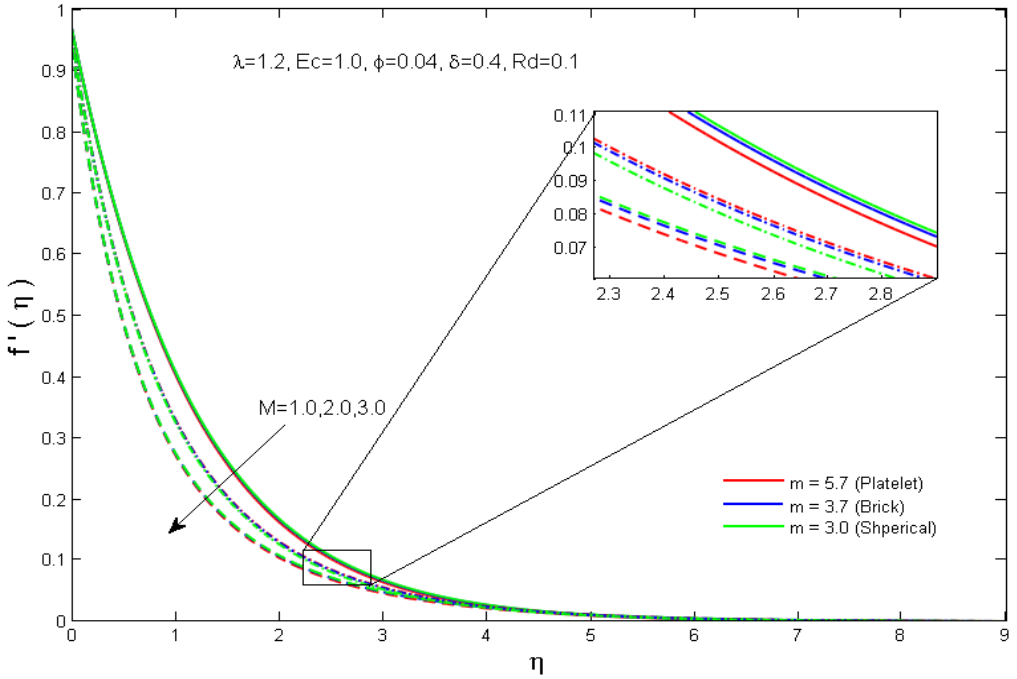

Figure 4.4: Variations in the Velocity with respect to M.

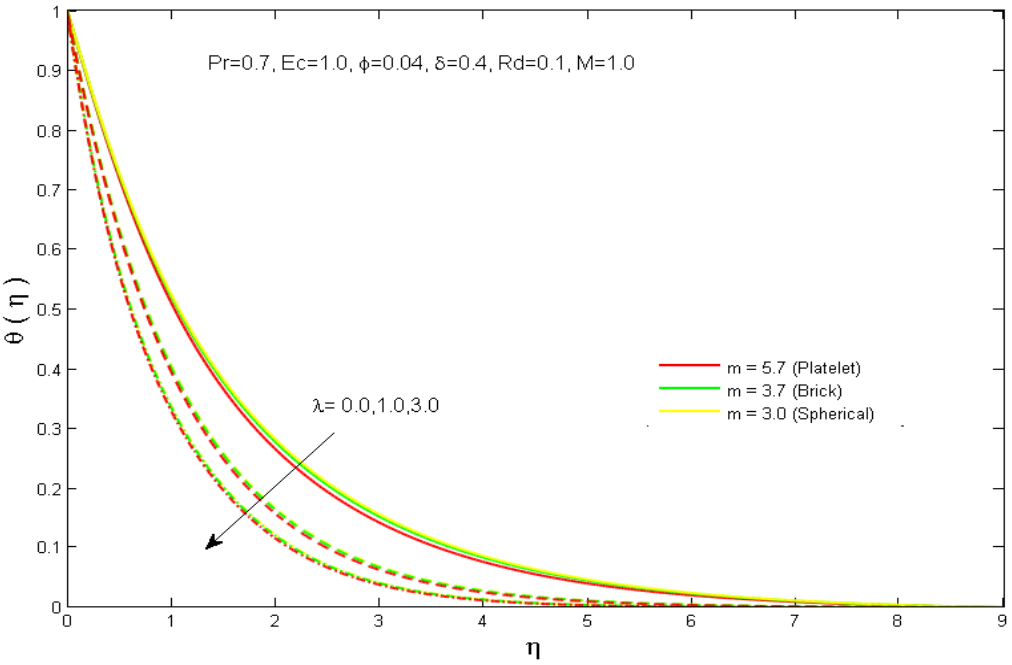

Figure 4.5: Variations in the Temperature with respect to λ.

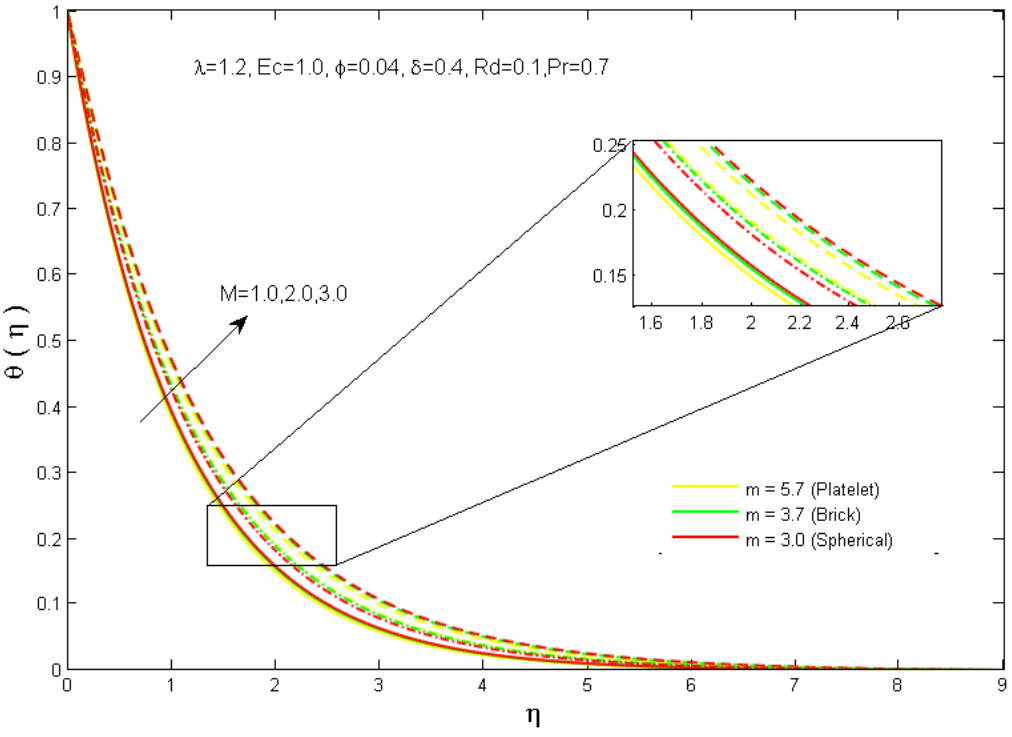

Figure 4.6: Variations in the Temperature with respect to M.

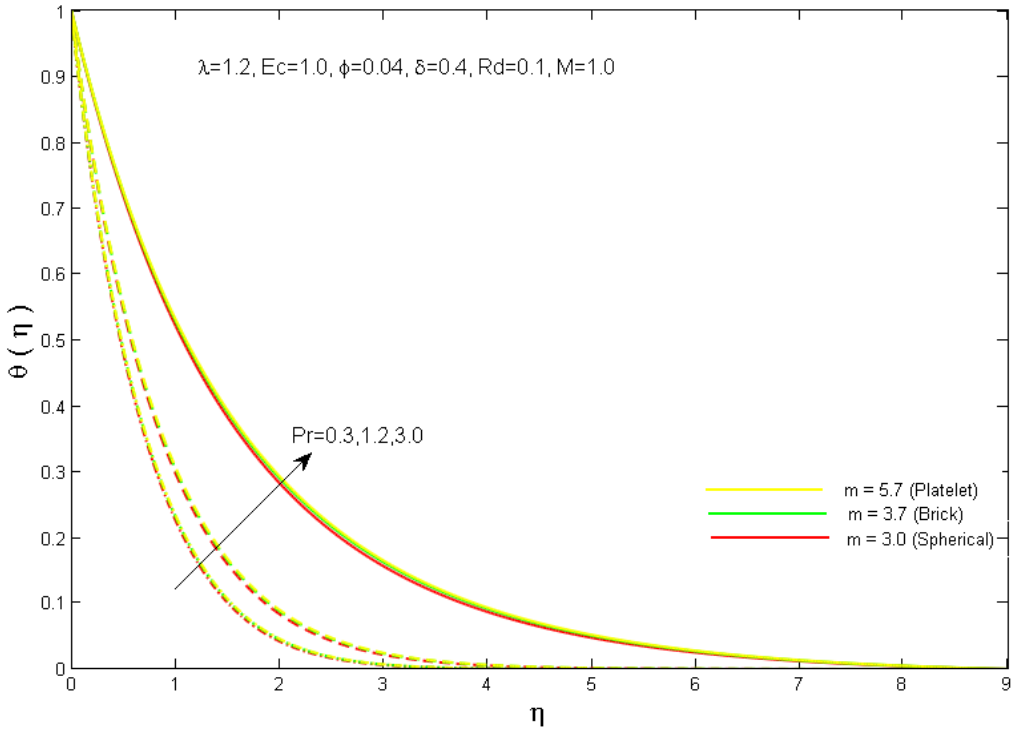

Figure 4.7: Variations in the Temperature with respect to Pr.

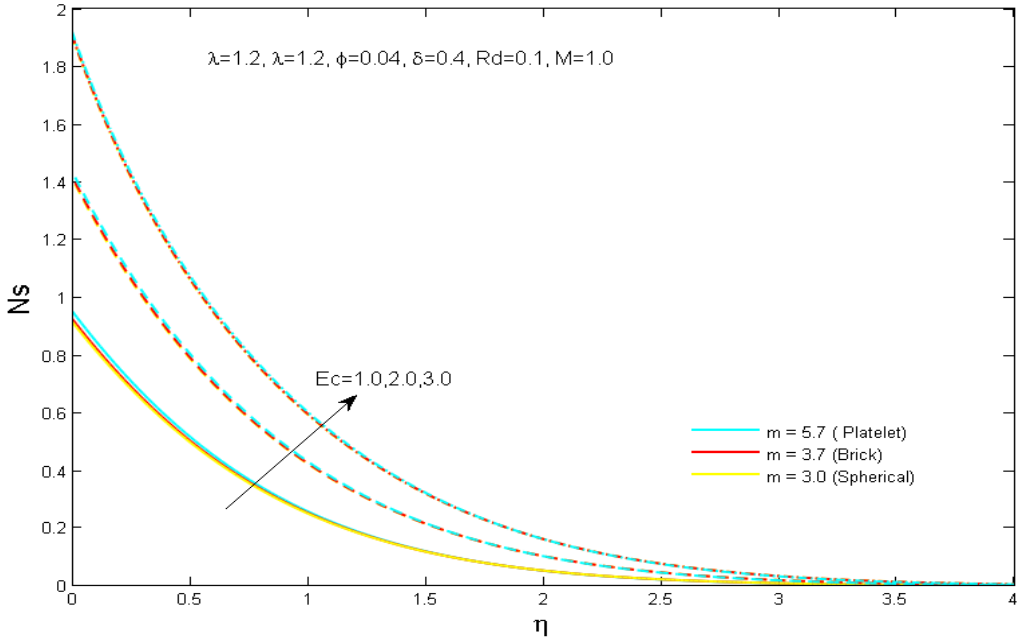

Figure 4.8: Entropy generation with changing Ec values.

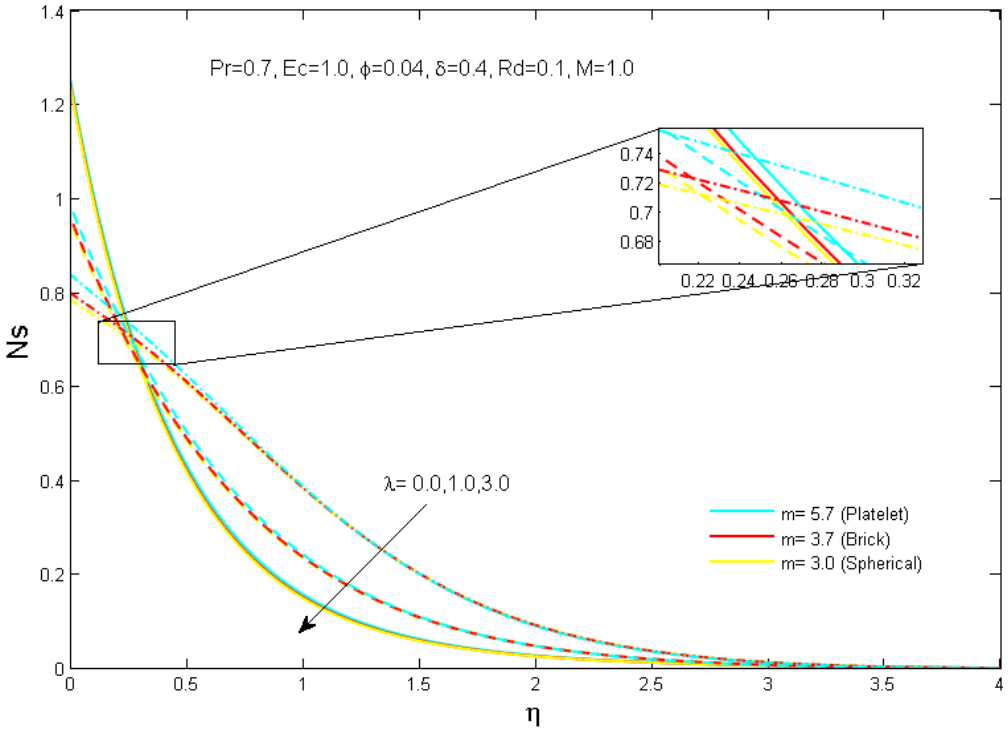

Figure 4. 9: Entropy generation with changing λ values.

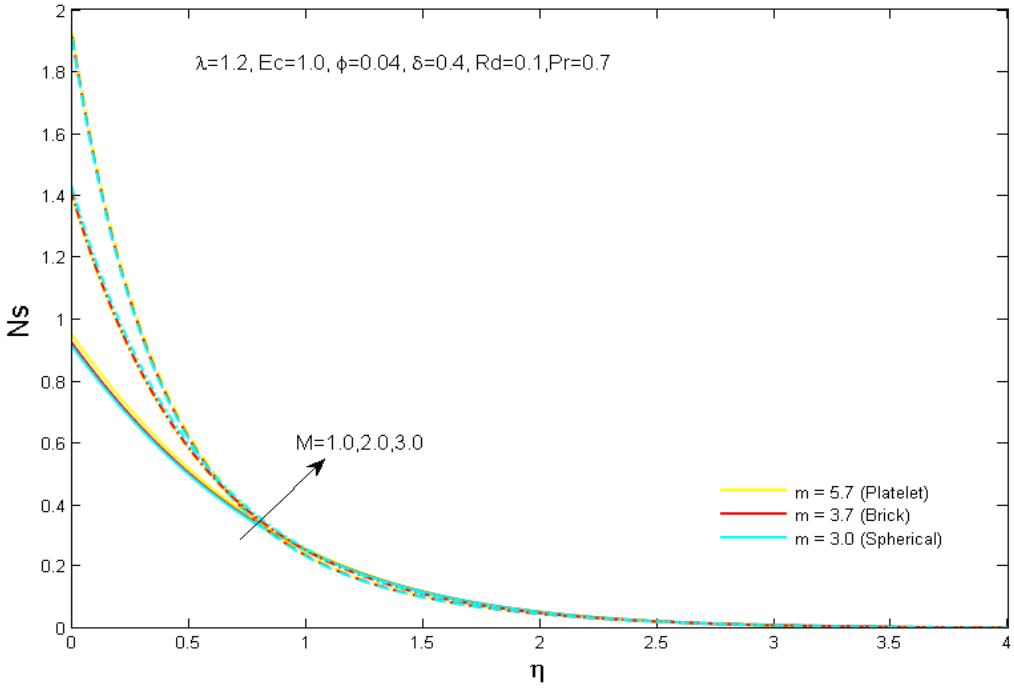

Figure 4.10: Entropy generation with changing M values.

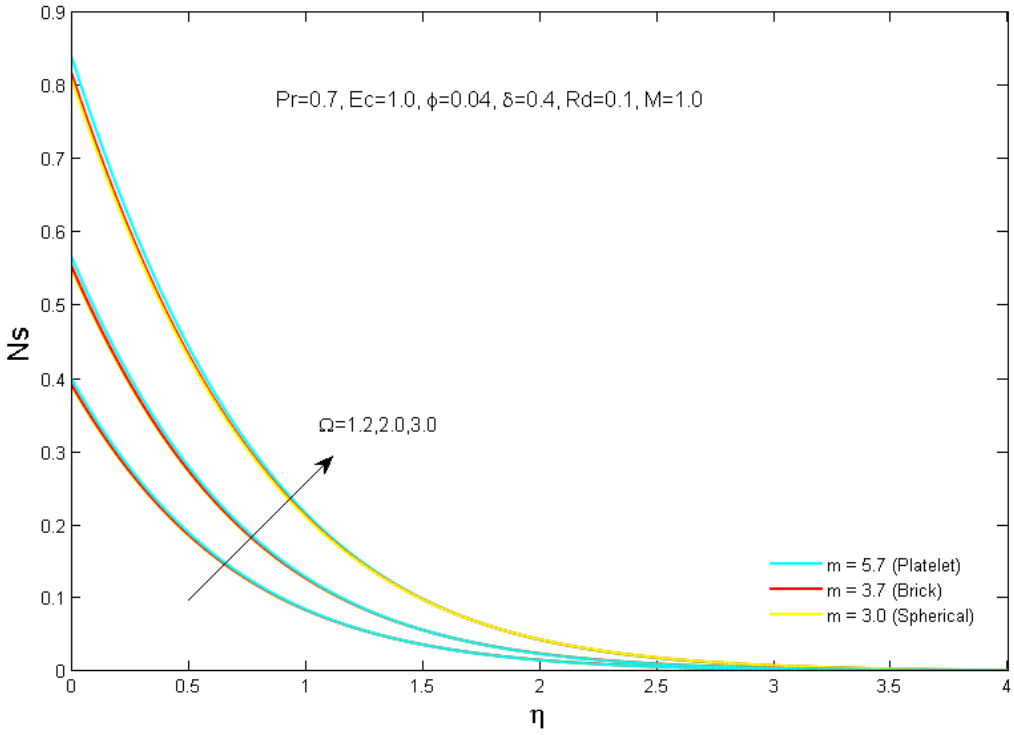

Figure 4.11: Entropy generation with changing Ω values.

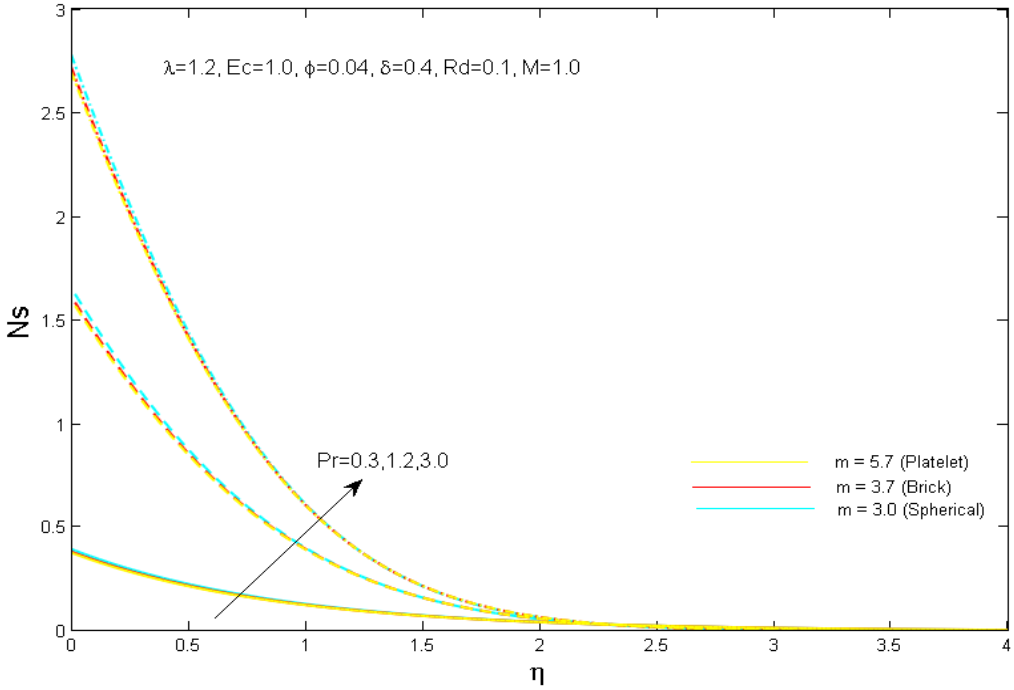

Figure 4.12: Entropy generation with changing Pr values.

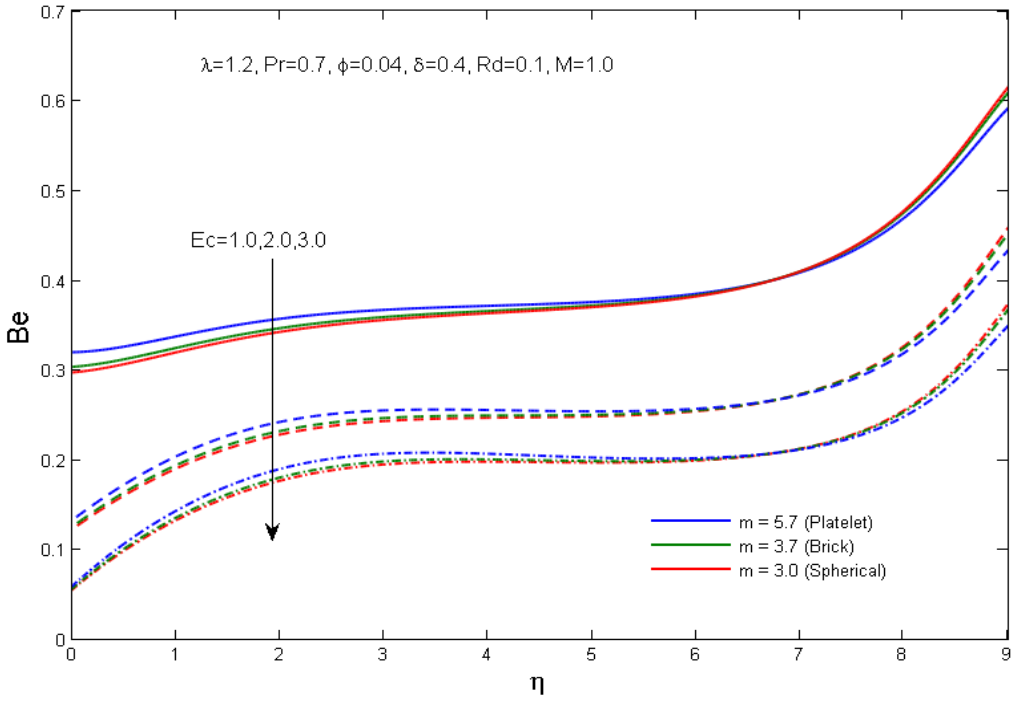

Figure 4.13: Bejan number with changing Ec values.

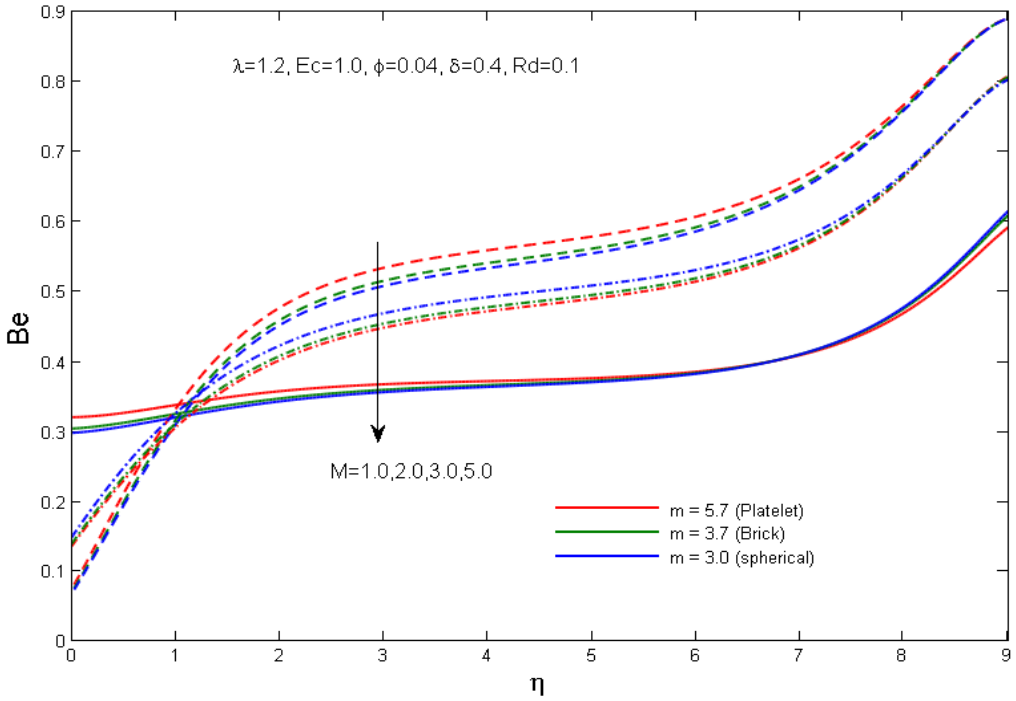

Figure 4.14: Bejan number with changing M values.

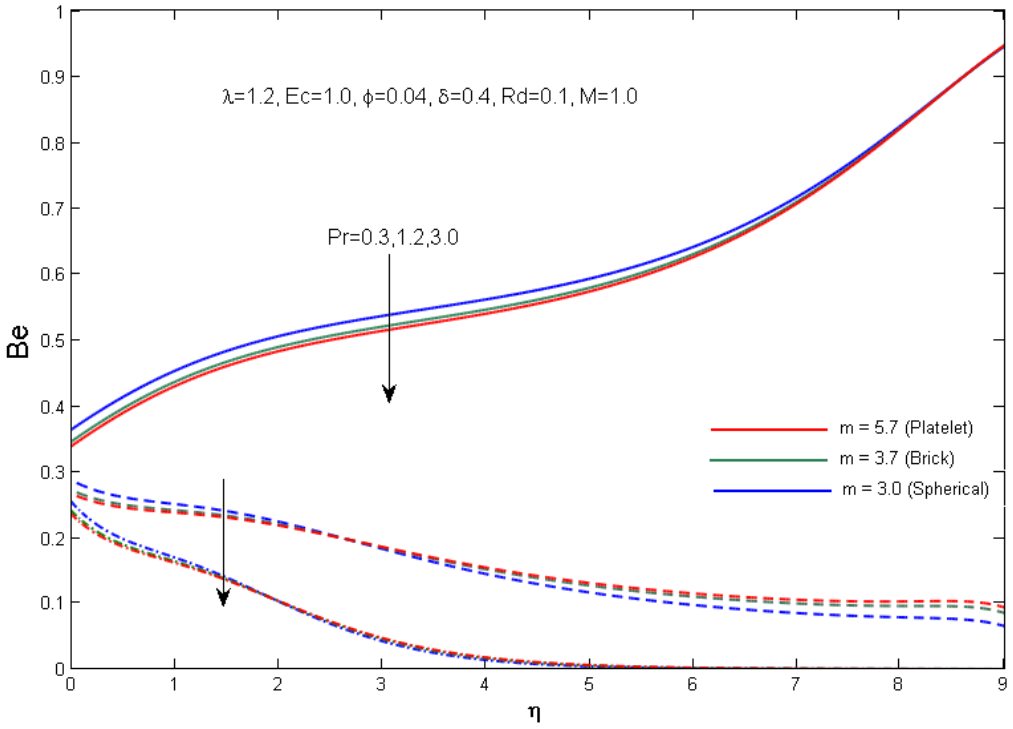

Figure 4.15: Bejan number with changing *Pr* values

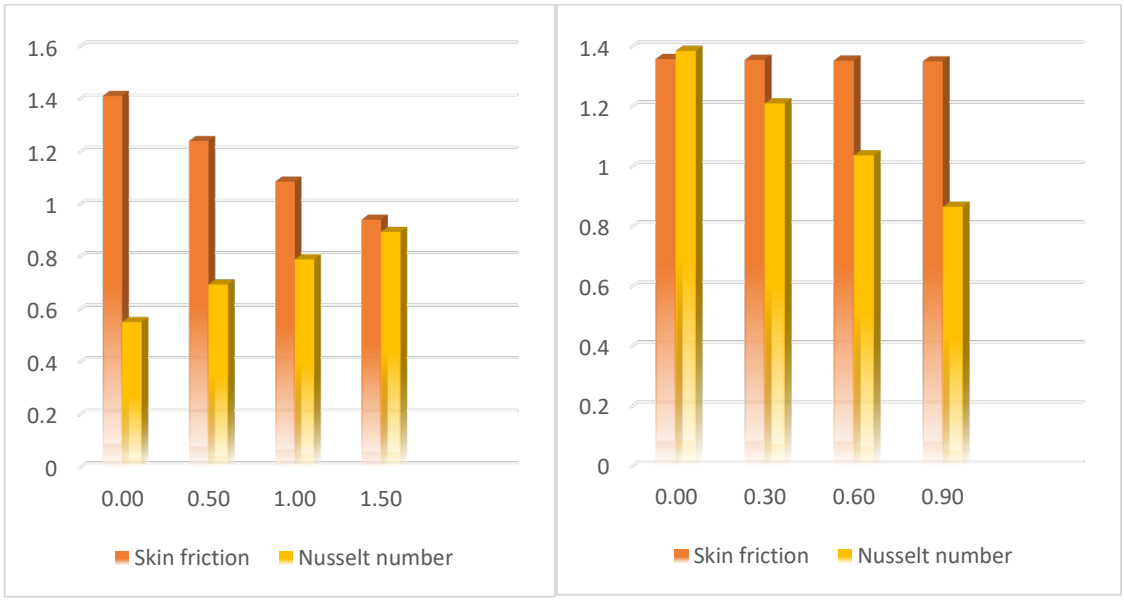

Figure.4.16: Outcomes of λ and Ec on skin friction and Nusselt number.

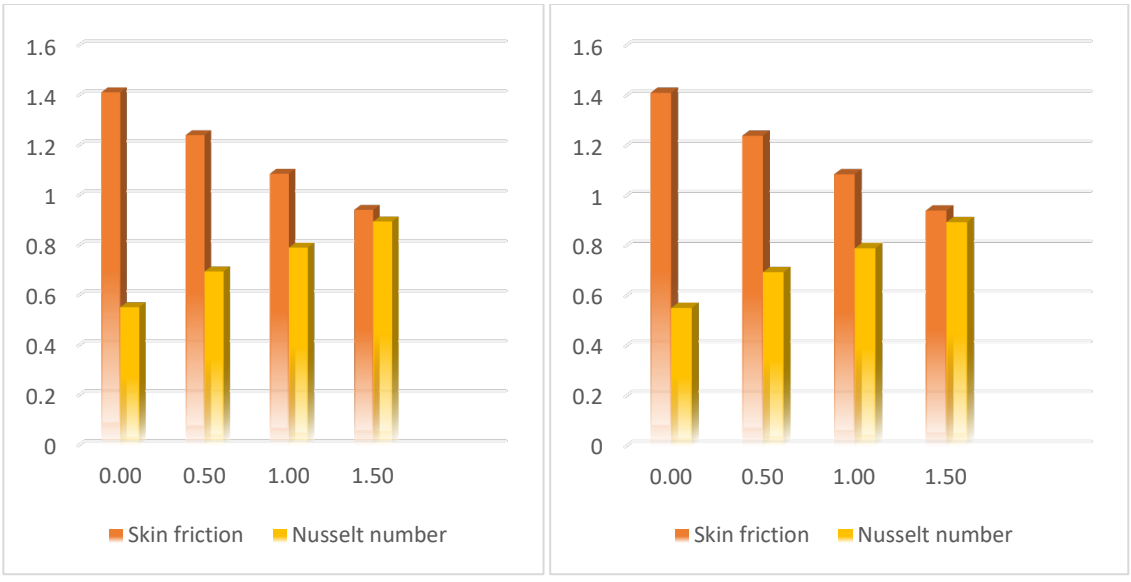

Figure.4.17: Outcomes of M and Pr on skin friction and Nusselt number.

CHAPTER 5

CONCLUSION

This chapter is an abstract of all the review and extension work results. Following are the points which are concluded:

- For the solution, the partial differential equations are transformed into ordinary differential equations using similarity transformation.
- Some dimensionless parameters are introduced, including Eckert numberEc, Entropy generation numberNs, Prandtl number Pr, Bejan numberBe, Reynold number Re and Grashof numberGr.
- KKL model is used to contact the nanofluid-containing nanoparticles along with the shape effects, including $m = 5.7$ (Platelet), $m = 3.7$ (Brick), and $m = 3.0$ (Spherical).
- It is noticed that the fluid motion decreases with the increase of Magnetic parameter M and increase in the increase of buoyancy parameter λ within the boundary layer.
- Amplification in nanoparticles, thermal boundary layer rise with an increase of Magnetic field M and Eckert numberEc. At the same time, with the variation of convective parameter λ and Prandtl number Pr there is a detection of decreasing.
- Entropy generation shows a massive boost with the rise of magnetic parameter M and Eckert number Ec, whereas reduction is seen as temperature ratio and thermal convective parameter rise.

- The Bejan number Be increases by ascending values of Prandtl number Pr and Eckert number Ec and behavior is opposite by ascending values of the magnetic parameter and buoyancy/convective parameter.
- The evaluation of Nusselt number Nu_x, skin friction C_f, and local Reynolds number Re_x increase with the increase of Prandtl number Pr and decrease with the decrease of Magnetic field parameter M and Eckert number Ec.
- The friction in fluid and magnetic irreversibility control the convection irreversibility close to the surface of stretching sheet as the magnetic field parameter increases and opposite results are observed for nanoparticle volume in Temperature.

REFERENCES

[1] A. Bejan, Second-Law Analysis in Heat Transfer and Thermal Design,Advances in Heat Transfer (1982) 1-58.

[2] A. Bejan, Entropy generation minimization: The new thermodynamics of finite-size devices and finite-time processes, Journal of Applied Physics, (1996) 1191-1218

[3] Y. A. Cengel, J. M. Cimbala and A. J. Ghajar, in Fundamentals of thermal-fluid sciences, McGraw Hill New York (2018) 703.

[4] L. Erbay, M. Ercan, B. Sülüs and M. Yalçÿn, Entropy generation during fluid flow between two parallel plates with moving bottom plate, Entropy (2003) 506-518.

[5] O. Makinde and E. Osalusi,Second Law Analysis of Laminar Flow In A Channel Filled With Saturated Porous Media,Entropy (2005) 148-160.

[6] K. Hooman and A. Ejali, Second law analysis of laminar flow in a channel filled with saturated porous media: A numerical solution (2005) 300-307.

[7] G. Komurgoz, A. Arikoglu and I. Ozkol, Analysis of the magnetic effect on entropy generation in an inclined channel partially filled with a porous medium, Numerical Heat Transfer, Part A: Applications (2012) 786-799.

[8] M. Rashidi, S. Abelman and N. F. Mehr, Entropy generation in steady MHD flow due to a rotating porous disk in a nanofluid, International Journal of Heat and Mass Transfer (2013) 515-525.

[9] A. S. Butt and A. Ali, Entropy effects in hydromagnetic free convection flow past a vertical plate embedded in a porous medium in the presence of thermal radiation,The European Physical Journal Plus (2013) 128.

[10] M. Afridi, M. Qasim, I. Khan, S. Shafie and A. Alshomrani, Entropy generation in magnetohydrodynamic mixed convection flow over an inclined stretching sheet, Entropy (2016) 19.

[11] M. I. Khan, S. Ullah, T. Hayat, M. Waqas, M. I. Khan and A. Alsaedi, Salient aspects of entropy generation optimization in mixed convection nanomaterial flow, International Journal of Heat and Mass Transfer (2018) 1337-1346.

[12] M. Sheikholeslami, M. Jafaryar, J. A. Ali, S. M. Hamad, A. Divsalar, A. Shafee, T. Nguyen-Thoi and Z. Li, Simulation of turbulent flow of nanofluid due to existence

of new effective turbulator involving entropy generation, Journal of Molecular Liquids (2019) 111283.

[13] Choi and S.U.S, Enhancing thermal conductivity of fluids with nanoparticles, Argonne National Laboratory (1995).

[14] A. A. Al-Rashed, K. Kalidasan, L. Kolsi, R.Velkennedy, A. Aydi, A. K. Hussein and E. H. Malekshah, Mixed convection and entropy generation in a nanofluid filled cubical open cavity with a central isothermal block International Journal of Mechanical Sciences (2018) 362-375.

[15] M. Sheikholeslami, M. Jafaryar, A. Shafee, Z. Li and R.-u. Haq, Heat transfer of nanoparticles employing innovative turbulator considering entropy generation, International Journal of Heat and Mass Transfer (2019) 1233-1240.

[16] T. Aziz, A. Aziz and C. Khalique, Exact solutions for stokes' flow of a non-newtonian nanofluid model: A lie similarity approach, Zeitschrift für Naturforschung A (2016) 621-630.

[17] S. Qayyum, T. Hayat and A. Alsaedi, Thermal radiation and heat generation/absorption aspects in third grade magneto-nanofluid over a slendering stretching sheet with newtonian conditions, Physica B: Condensed Matter (2018) 139-149.

[18] Aziz and Asim, Unsteady MHD slip flow of non Newtonian power-law nanofluid over a moving surface with temperature dependent thermal conductivity, Discrete & Continuous Dynamical Systems - S (2018) 617-630.

[19] Z. Mehmood, R. Mehmood and Z. Iqbal, Numerical investigation of micropolar Casson fluid over a stretching sheet with internal heating, Communications in Theoretical Physics (2017) 443.

[20] Z. Iqbal, R. Mehmood, E. Azhar and Z. Mehmood, Impact of inclined magnetic field on micropolar Casson fluid using Keller Box Algorithm, The European Physical Journal Plus (2017) 132.

[21] U. Rashid and A. Ibrahim, Impacts of nanoparticle shape on Al203-water nanofluid flow and heat transfer over a non-linear radically stretching sheet,Advances in Nanoparticles (2020) 23-39.

[22] T. KO and K. TING, Optimal Reynolds number for the fully developed laminar forced convection in a helical coiled tube, Energy (2006) 2142-2152.

[23] M. R. Hajmohammadi, G. Lorenzini, O. J. Shariatzadeh and C. Biserni, Evolution in the design of V-shaped highly conductive pathways embedded in a heat-generating piece, Journal of Heat Transfer (2015) 137.

[24] G. Xie, Y. Song, M. Asadi and G. Lorenzini, Optimization of pin-fins for a heat exchanger by entropy generation minimization and constructal law, Journal of Heat Transfer (2015) 137.

[25] G. Lorenzini and S. Moretti, Bejan's constructal theory and overall performance assessment: The global optimization for heat exchanging finned modules, Thermal Science (2014) 339-348.

[26] A. Pouzesh, R. M. Hajmohammadi and S. Poozesh, Investigations on the internal shape of constructal cavities intruding a heat generating body, Thermal Science (2015) 609-618.

[27] M. R. Hajmohammadi, A. Campo, S. S. Nourazar and A. M. Ostad, Improvement of forced convection cooling due to the attachment of heat sources to a conducting thick plate, Journal of Heat Transfer (2013) 135.

[28] M. Govindaraj, N. V. Ganesh, B. Ganga and A. A. Hakeem, Entropy generation analysis of Magneto hydrodynamic flow of a nanofluid over a stretching sheet, Journal of the Egyptian Mathematical Society (2015) 429-434.

[29] A. Shafee, M. Jafaryar, A. I. Alsabery, A. Zaib and H. Babazadeh, Entropy generation of nanomaterial through a tube considering Swirl Flow Tools, Journal of Thermal Analysis and Calorimetry (2020) 1597-1612.

[30] J. Koo and C. Kleinstreuer, A new thermal conductivity model for nanofluids, Journal of Nanoparticle Research (2004) 577-588.

[31] J. Li, C. Kleinstreuer and Y. Feng, Computational analysis of thermal performance and entropy generation of nanofluid flow in microchannels,"ASME 2012 Third International Conference on Micro/Nanoscale Heat and Mass Transfer (2012).

[32] N. Dalir, M. Dehsara and S. S. Nourazar, Entropy analysis for magnetohydrodynamic flow and heat transfer of a Jeffrey nanofluid over a stretching sheet, Energy (2015) 351-362.

[33] G. Shit, R. Haldar and S. Mandal, Entropy generation on MHD flow and convective heat transfer in a porous medium of exponentially stretching surface saturated by nanofluids, Advanced Powder Technology (2017) 1519-1530.

[34] T. Hayat, M. I. Khan, S. Qayyum and A. Alsaedi, Entropy generation in flow with silver and copper nanoparticles, Colloids and Surfaces A: Physicochemical and Engineering Aspects, (2018) 335-346.

[35] N. V. Ganesh, A. J. Chamkha, Q. M. Al-Mdallal and P. Kameswaran, Magneto-marangoni nano-boundary layer flow of water and ethylene glycol based γ nanofluids with non-linear thermal radiation effects, Case Studies in Thermal Engineering (2018) 340-348.

[36] O. Makinde and P. Olanrewaju, Buoyancy effects on thermal boundary layer over a vertical plate with a convective surface boundary condition, Journal of Fluids Engineering (2010) 132.

[37] A. Mahdy, Unsteady mixed convection boundary layer flow and heat transfer of nanofluids due to stretching sheet, Nuclear Engineering and Design, (2012) 248-255.

[38] R.L.Hamilton and O.K.Crosser, Thermal conductivity of heterogeneous two-component systems, Industrial & Engineering Chemistry Fundamentals (1962) 187-191.

Entropy analysis due to free convection flow along a vertical surface

ORIGINALITY REPORT

16%	10%	12%	4%
SIMILARITY INDEX	INTERNET SOURCES	PUBLICATIONS	STUDENT PAPERS

PRIMARY SOURCES

1	Submitted to Higher Education Commission Pakistan Student Paper	2%
2	www.mdpi.com Internet Source	1%
3	Ferruh Erdogdu, Mustafa Tutar. "A computational study for axial rotation effects on heat transfer in rotating cans containing liquid water, semi-fluid food system and headspace", International Journal of Heat and Mass Transfer, 2012 Publication	1%
4	researchspace.ukzn.ac.za Internet Source	1%
5	cyberleninka.org Internet Source	1%
6	aip.scitation.org Internet Source	<1%